Standard Aeronautical Index No.

ON THE MAIN SPRAY GENERATED BY PLANING SURFACES

by

DANIEL SAVITSKY
and
JOHN P. BRESLIN

Experimental Towing Tank
Stevens Institute of Technology

S.M.F. Fund Paper
No. FF-18

IAS Member Price - $0.75
Price to Nonmembers - $1.25

Received - January 1958

A Sherman M. Fairchild Publication Fund Paper

By the

INSTITUTE OF THE AERONAUTICAL SCIENCES

2 EAST 64th STREET NEW YORK 21, N. Y.

Title

DISCLAIMER NOTICE

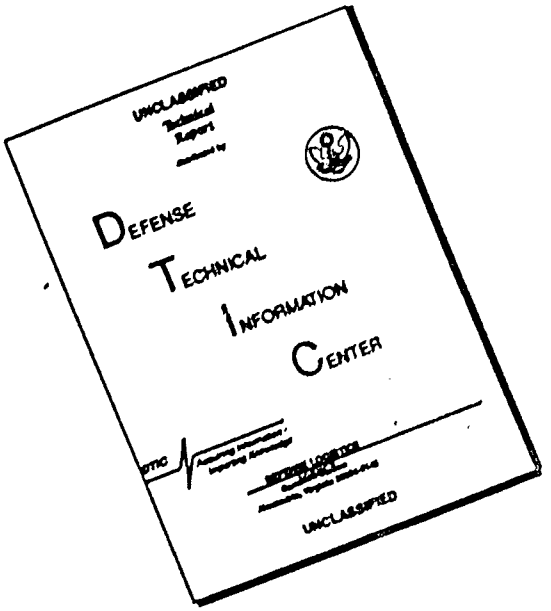

THIS DOCUMENT IS BEST QUALITY AVAILABLE. THE COPY FURNISHED TO DTIC CONTAINED A SIGNIFICANT NUMBER OF PAGES WHICH DO NOT REPRODUCE LEGIBLY.

EXPERIMENTAL TOWING TANK
STEVENS INSTITUTE OF TECHNOLOGY
HOBOKEN, NEW JERSEY

ON THE MAIN SPRAY GENERATED BY PLANING SURFACES

by

Daniel Savitsky

and

John P. Breslin

PREPARED UNDER U.S. NAVY, OFFICE OF NAVAL RESEARCH
CONTRACT NO. Nonr 263(10)
(E.T.T. PROJECT NO. FX 1700)

January 1958

Report No. 678

TABLE OF CONTENTS

SUMMARY

Analytical and experimental model studies were made at the Stevens Institute of Technology, Experimental Towing Tank (ETT) in order to determine the origin and dependence upon the basic planing parameters of the main spray associated with prismatic planing hulls. It was found that the main spray originates locally at the stagnation line intersection with the chine and that the water contained in the spray comes from a strip of undisturbed surface fluid lying ahead of and parallel to the chine over a width approximately 0.10 beams on either side of the chine line. The maximum spray height was found to be proportional to the square of the planing velocity, increased almost linearly with increasing trim angle, did not vary strongly with deadrise angle, achieved a maximum height at a deadrise angle of 10 degrees, and was independent of aspect ratio in the chines-wetted planing condition. Small vertical spray strips were very effective in causing considerable reductions in spray height. Horizontal chine flares were ineffective in reducing the spray height.

NOMENCLATURE

b	beam of planing surface
C_v	speed coefficient $V/\sqrt{gb}$
d	depth of chine strip below chine line
g	acceleration of gravity
p	pressure
p_s	stagnation pressure
R	radius of curvature
t	thickness of the stream tube
V	resultant fluid velocity
V_n	velocity component normal to stagnation line
V_s	velocity component parallel to the stagnation line

x	horizontal distance along body axis
y	transverse distance in body axis
α	angle between stagnation line and whisker spray measured in plane of bottom
β	deadrise angle
δ	spray thickness
η	lateral position of maximum height of main spray blister outboard of chine
γ	angle between spray sheet and planing surface
λ	mean wetted length beam ratio, ℓ_m/b
ℓ	total length of planing surface
ℓ_1	distance of stagnation point ahead of trailing edge of planing surface
ℓ_2	distance of stagnation point behind the leading edge of planing surface
ℓ_m	mean wetted length
ω	$\tan^{-1} dy/dx$
ρ	mass density of fluid
σ	surface tension of fluid
τ	trim angle
ζ	maximum height of main spray blister above level water surface

INTRODUCTION

This report presents the results of a model study of the phenomena of the main or blister spray generated by planing hulls. Motivation for this work stemmed from the importance of such sprays as are produced by seaplanes during take-off and landing. It always has been a problem for the seaplane designer to arrange the wing, tail and engine locations to

minimize the wetting of such members by the planing spray. Impingement of a heavy spray on the wings, particularly upon the flaps, can and has produced structural damage. With the advent of jet-powered seaplanes, it is particularly important that spray be so controlled as to prevent ingestion into the jet engines of water which can easily extinguish combustion or lead to corrosion of turbine blades.

Present-day practice in design of seaplanes seeks to provide a control on the spray by means of spray dams which are essentially flanges into which the hull is faired at the chine. The dams direct the water downward at the juncture of the chine and water surface. Small-scale tests have been conducted with a model of the specific seaplane under consideration in order to determine the effectiveness of the chine configurations in reducing the spray configuration with respect to the hull. Such experimentation usually has been on a design-to-design basis and, although materially assisting in the solution of specific spray problems, has contributed little to an understanding of the flow pattern, its origin, and how it depends upon speed, trim and the geometry of a body. Inasmuch as a basic systematic study of seaplane spray generation is lacking, a combined theoretical and experimental investigation was undertaken to provide some insight into the mechanism of the generation of the main spray and how its geometry varies with planing conditions and the shape of the planing body.

This report begins with a description of the basic types of spray formations produced by planing surfaces and how their qualitative behavior and generation may be accounted for theoretically. The experimental work undertaken is described next and the test results are presented in a form which shows the dependence of the coordinates of the maximum height of the main spray upon the speed coefficient and angles of trim and deadrise. The effectiveness of simple spray strips along the chine is determined from systematic tests.

This work, which has been conducted at the Experimental Towing Tank, Stevens Institute of Technology (ETT), has been supported by the Mechanics Branch, Office of Naval Research under Contract Nonr 263(10). This study was designated as Project No. NR-1700 at ETT.

BASIC CONCEPT OF SPRAY GENERATION

General Considerations

It is common knowledge that large distortions of a fluid surface occur near the leading edge of wetted areas of bodies which plane upon or pierce the water surface at high speeds. These high-speed water distortions generally lead to the formation of spray. At low speeds the water action near the bow takes the form of a wave which is in continuous contact with the body surface and neighboring fluid. At higher speeds the flow about the bow fails to cling to the surface as a wave and separates from it, thus forming a locally ventilated flow. Depending upon the shape of the leading edge, this ventilation may be preceded or followed by a rupturing of the flow into two parts. One part forms the spray which moves out and upward, while the other remains as the main body of the flow field. The basic reason for such a strong reaction is the presence of a stagnation line in the immediate vicinity of the free surface. A stagnation line is a locus of points on a body along which the flow is divided into two parts and on which the maximum pressure is developed from the bringing to rest an important component of the free stream velocity, V. At low V, the presence of this stagnation line will cause a local "bump" or swelling of the free surface and will contribute to the generation of a wave train downstream or aft of the body. As the planing surface velocity, V, is increased, the fluid above the stagnation streamline will move upward and outward with increasing force until the layer tears away. Determination of the velocity which initiates this transition can be explained by taking, as example, the case of an obstacle placed close to the fluid-air interface as is shown in the adjacent sketch.

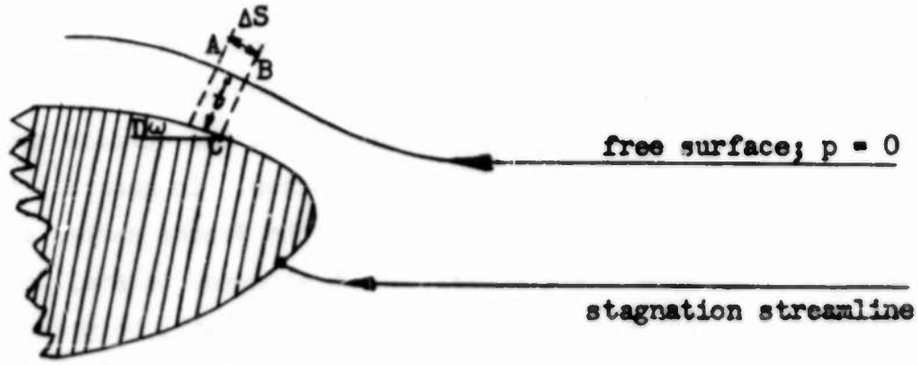

leading edge of body
over which pressure
is positive

The forces acting on the element ABCD are considered to be: 1) the reaction from the body, 2) the surface tension, and 3) gravity. The equation of motion along the normal to the body then is

$$p(s)(\Delta S) - 2\sigma \frac{d^2y}{dx^2}(\Delta S) - \rho g t(\Delta S)\cos\omega = -\rho t\,\Delta S\,\frac{V^2}{R} \quad , \qquad (1)$$

provided the frictional forces are neglected. If the thin layer of water rounding the obstacle is to detach and thus ventilate, the pressure along DC must fall to zero. The critical velocity then is given by

$$V^2_{cr} = 2R\,\frac{\sigma}{\rho t}\,\frac{d^2y}{dx^2} + gR\cos\omega \quad . \qquad (2)$$

The general expression for radius of curvature is

$$R\,\frac{d^2y}{dx^2} = \left(1 + \left(\frac{dy}{dx}\right)^2\right)^{3/2} \quad . \qquad (3)$$

Substituting Equation (3) into Equation (2) results in

$$V^2_{cr} = \frac{2\sigma}{\rho t}\left[1 + \left(\frac{dy}{dx}\right)^2\right]^{3/2} + gR\cos\omega \quad . \qquad (4)$$

Inasmuch as the surface tension of water is small (about 0.00512 lb./ft.), the coefficient of the first term on the right-hand side of Equation (4) (0.00512/t) can be large, relative to the second term, only for very small bodies. For geometrically similar obstacles, the importance of the first term diminishes linearly with size (since t increases with size), whereas the last term grows linearly with size. Consequently, the surface tension plays virtually no role in the flow about large bodies. In general, then, the onset of spray may be expected to depend upon the Froude number and the Weber number so that some scale effect can be expected in small model tests in which only the Froude number is preserved. As will be presently seen, the thickness, t, of the fluid layer which is skimmed off into spray by a flat planing surface is indeed small so that it is quite possible for surface tension to influence the generation of spray and the shape of the spray sheet after it leaves the hull.

Spray Generated by a Two-Dimensional Flat Planing Plate

The local flow pattern about a flat plate planing on the surface of a fluid has been treated by Wagner[1] and more completely by A.E. Green[2] using the two-dimensional free-streamline theory. For present purposes it will be sufficient merely to use some of their results to illustrate the theoretically predicted flow pattern about a flat planing surface.

Wagner's mathematical model is considered first to illustrate the fact that the spray thickness is small compared to a characteristic dimension of the body. Wagner considered a plate whose length above the calm water intersection is infinite as shown in the following sketch.

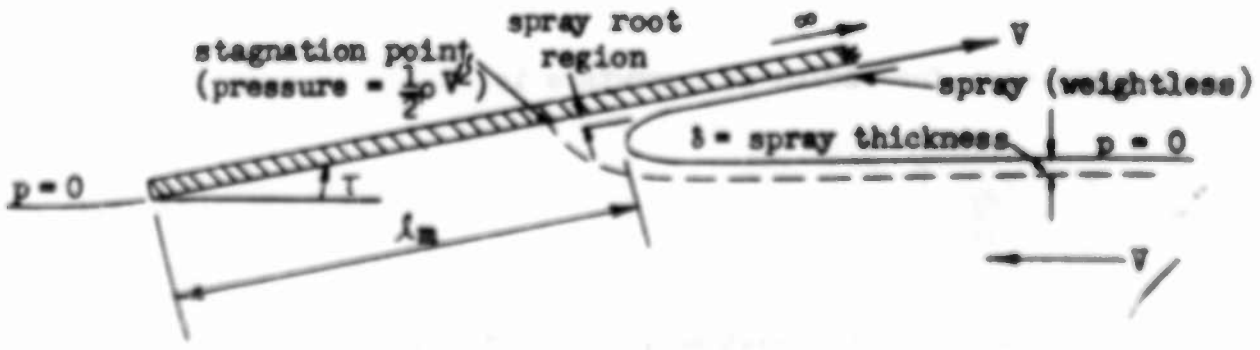

Wagner's Two-Dimensional Spray Configuration

Using Wagner's solution, which applies to speeds such that the inertia forces are much larger than the gravity force, Equation (29) of Reference 3 can be used to approximate the spray thickness, δ , in a fraction of the wetted length (ℓ_m) measured to the spray root as:

$$\frac{\delta}{\ell_m} \approx \frac{\pi \tau^2}{4 + 2\pi\tau} \qquad (\text{for } \tau << 1.0) \quad , \tag{5}$$

where τ is the trim angle in radians. Thus, for a trim angle of 12 degrees, δ is only about 2.5 percent of ℓ_m and is directed upward at the trim angle τ. However, this initial trajectory angle of the spray depends upon the initial extent of the upper end of the plate above the undisturbed free surface as shown theoretically by Green[2] who considered both plates of finite and infinite length planing on fluids of infinite and finite depth.

The adjacent sketch shows the flow pattern for the case of a plate of finite length planing in a fluid of infinite depth.

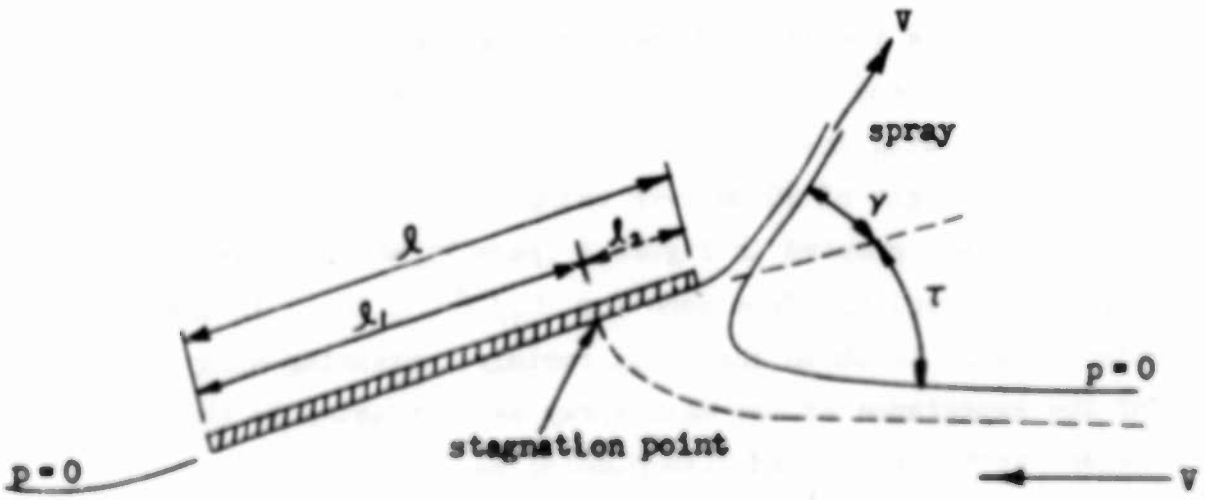

Green's Two-Dimensional Spray Configuration
For Finite Length Planing Plate

When ℓ is made infinite in such a way that ℓ_1 is fixed and $\ell_2 \longrightarrow \infty$, Green's results reduce to Wagner's. But for ℓ_2 finite the spray trajectory angle, γ , is considerably different from the trim angle, τ. Green's solution enables one to compute the flow and forces acting on a plate for any near surface submergence so that the case of a fully venti-

lated plate can be computed. This is illustrated in the following sketch.

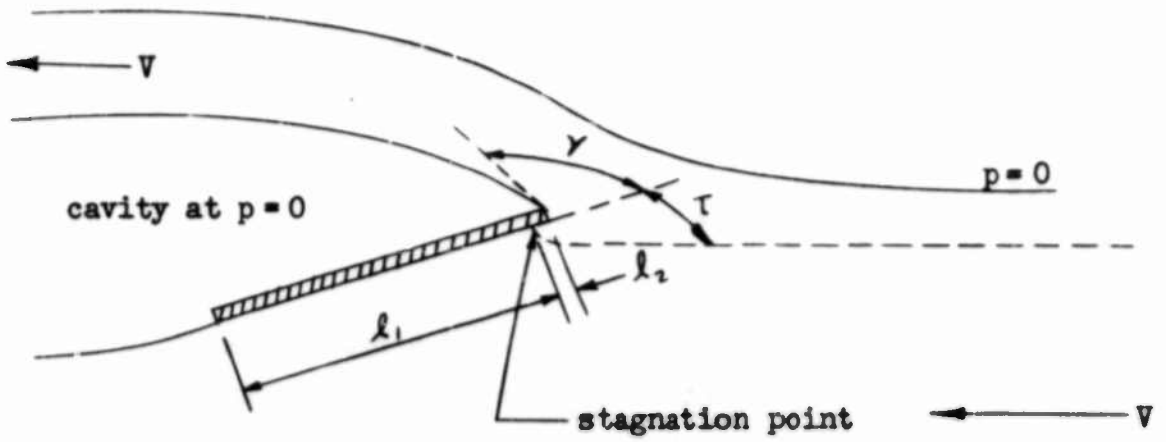

Fully Ventilated Submerged Flat Planing Plate

For this case it is evident that the spray thickness is large and the angle γ is many times τ, approaching, in fact, the supplement of τ. The important fact to note is that as a plate is immersed in a fluid, say at constant trim angle, the stagnation point moves closer to the upper end of the plate. At the same time the width of the stream tube, formed by the stagnation streamline and the free surface, thickens and, at a particular position, the inertia* of the spray becomes so great that the divided flow begins to bend around the top edge of the plate. The variation of the angle γ with the position of the stagnation line has been evaluated for a trim angle of 30 degrees using Green's theoretical expressions. The results are graphed in Figure 1 (page 30) which shows that the angle γ departs appreciably from zero for $\ell_1/\ell > 0.60$. In the following section it will be shown that this rapidly increasing spray angle accounts for the appearance of the main spray as contrasted to the so-called "whisker" spray associated with planing surfaces.

---

*It is to be noted that the fluid is endowed with mass density so that inertia forces exist but that gravity is neglected.

Spray Generated by a Three-Dimensional Prismatic Planing Body

In order to describe the two basic spray shapes associated with planing forms and the hydrodynamic flow processes which lead to the generation of these sprays it is necessary to examine the geometry of a simple, constant deadrise planing body and the associated free water surface as shown in the following sketch.

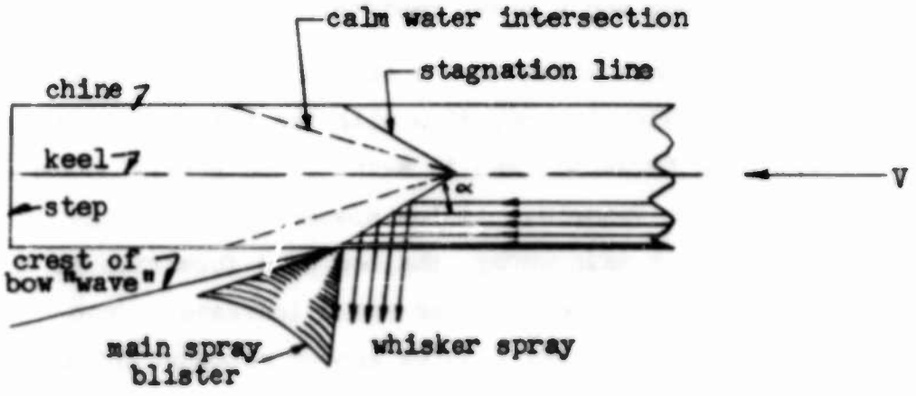

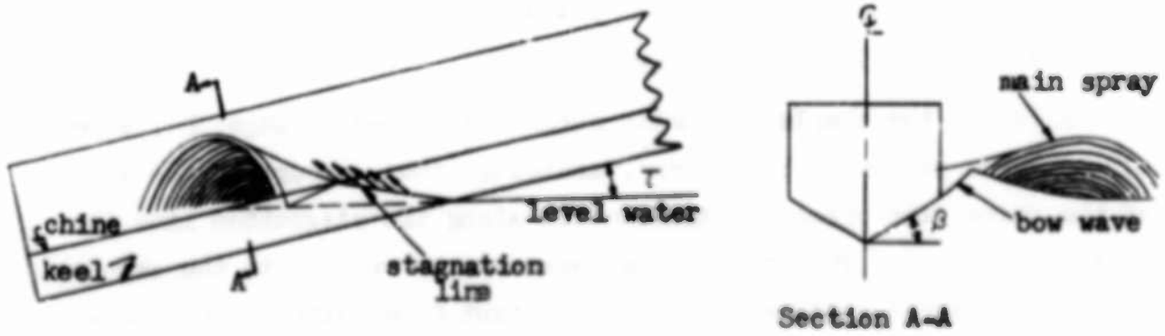

A pile-up of water ahead of the calm-water intersection with the bottom takes place at the forward edge of the wetted planing area. According to theoretical and experimental results (References 1 and 4), the actual wetted width is essentially $\pi/2$ times the wetted width defined by the level water intersection with the bottom. In the immediate vicinity of the wetted leading edge, a stagnation line of high pressures exists. The angle of the stagnation line relative to keel can be geometrically established from a knowledge of the deadrise, trim and $\pi/2$ wave rise factor. Two distinct spray patterns are shown in the previous sketch. One is the so-called

"whisker" spray which appears along the length of the stagnation line, and the other is the main spray which rises sharply from the side of the hull after originating in the vicinity of the stagnation line intersection with the chine. Characteristically, the whisker spray is a thin, light spray consisting of droplets of water. The main spray is a continuous blister of fluid in the form of a cone whose apex is in the vicinity of the stagnation line intersection with the chine. Both spray patterns are apparent in Figure 2 (page 31) which is a photograph of a 20 degree deadrise surface planing at a trim angle of eight degrees and a speed coefficient of 4.00.

Another free surface disturbance shown in the sketch on page 9 is a bow wave which originates at the chine intersection with the water surface. This bow wave is a divergent wave formation and is akin to the gravity waves which exist for normal displacement vessels. At low speeds, prior to the development of either the whisker or main spray, the bow wave formation is the only visible water surface disturbance. As the speed increases, droplets of whisker spray and a small main spray blister appear somewhat outside the crest of the bow wave. At high planing speeds the whisker and main spray formations become larger and wider so that they predominate and completely obscure the bow wave. For all planing speeds, the height of the crest of the bow wave is relatively small.

Considering the simple prismatic surface sketched on page 9 , experimental evidence presented by Smiley[5], indicates that, except in the vicinity of the chine, the pressure distribution along the stagnation line is essentially constant. This fact lends considerable support to the assumptions made by several writers that the resultant flow patterns in three-dimensional planing can be decomposed into two-dimensional components. Thus, in analogy to the aerodynamic treatment of flows over swept-back wings, the free stream velocity can be resolved into a component V_n normal to and a component V_s along the stagnation line as shown in the following sketch which is an enlargement of the leading edge of the wetted bottom area. The velocity components V_n and V_s are defined in terms of deadrise and trim angle by Pierson and Leshnover[6].

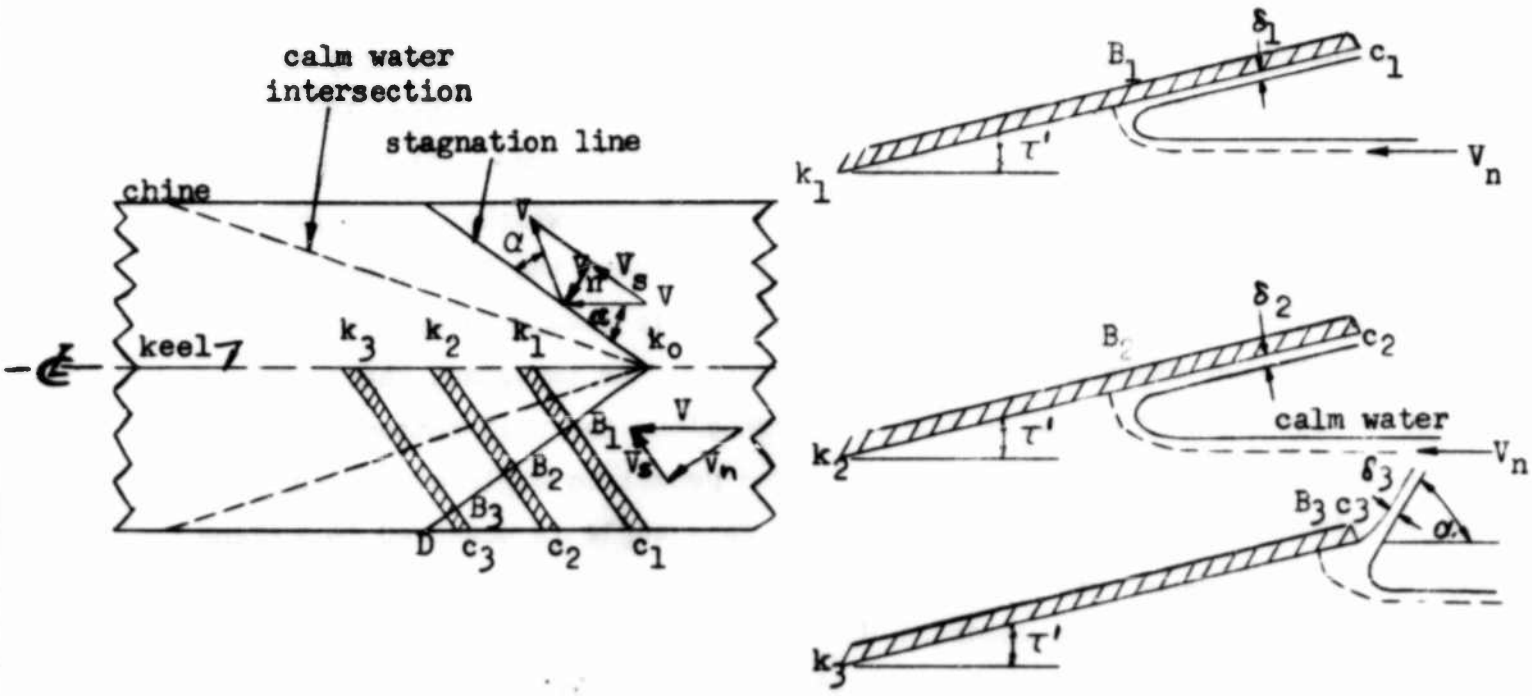

Since V_s is essentially constant along the stagnation line (as a consequence of the assumption of constant stagnation pressure and Bernoulli's equation), the flow in planes normal to the stagnation line (sections k-c) may be treated as two-dimensional flows. Hence, it can be assumed that the flow in section k-c is equivalent to the flow about a two-dimensional flat plate planing at an effective τ' and V_n. If the plane k-c is taken to be fixed in space and the planing surface is made to pass through this plane at a constant V, an examination of the changing flow patterns in the plane k-c will lead to a possible physical explanation for the generation of both the whisker and main sprays.

This can be explained by considering consecutive positions k_1c_1, k_2c_2 and k_3c_3 of the plane normal to the stagnation line. For positions k_1c_1 and k_2c_2, the effective two-dimensional flow is that of a semi-infinite flat plate as treated by Wagner[1] and discussed on page 6 of this report. In these planes a thin spray, δ, is generated and flows along the bottom surface making an effective angle τ' with respect to the calm water surface. Using the principles of similitude, the wetted length and spray thickness associated with these equivalent two-dimensional flat plates increase linearly with increasing distance kB. The effective two-dimensional planing velocity for a plane such as k_1c_1 is V_n and,

consequently, the spray velocity in this plane is V_n. In the actual three-dimensional flow pattern the velocity component V_s is added to the two-dimensional component V_n so that the resultant spray velocity is V and makes an angle $\alpha = \tan^{-1} V_n/V_s$ relative to the stagnation line. This resultant spray is the whisker spray previously described. It should be noted, from the previous sketch on page 11, that the whisker spray makes the same angle α with the stagnation line as does the free stream velocity V. This principle of "spray reflection" is developed analytically and demonstrated experimentally in Reference 6. An important characteristic of the whisker spray is that it flows along the hull bottom and leaves the chine at an angle which is equal to the geometric angle of the hull bottom relative to the level water surface. This angle is measured in a plane which is at an angle α to the stagnation line and normal to the bottom. For conventional trim and deadrise combinations, this hull bottom angle is usually small and, consequently, the whisker spray, which follows a ballistic trajectory after leaving the chine, does not achieve large heights above the water surface. Furthermore, since the whisker spray is composed of thin, light droplets of fluid it usually is controlled by moderate chine flares.

For normal planes near the chine terminus of the stagnation line, i.e., section k_3c_3, a sharp change in the two-dimensional flow pattern takes place primarily because the effective two-dimensional surface becomes a surface of finite length whose leading edge is in close vicinity to the stagnation line. In the inboard sections (k_1c_1, k_2c_2) the equivalent two-dimensional flows were taken as being similar to the Wagner semi-infinite flow solution and the resultant spray direction was shown to be tangent to the hull bottom. At the finite length outboard sections (k_3c_3) the equivalent two-dimensional flows are similar to those described by Green[2] (and on page 7 of this report) where the spray sheet bends around the leading edge of the planing surface and develops large initial trajectory angles upon leaving the surface.

Using Green's formulas, Figure 1 on page 30 has been prepared to show the variation in spray trajectory angle with a decreasing total length of planing surface. It can be seen that, for ratios of effective wetted length to total length less than .60, the spray trajectory angle is equal to the

trim angle of the planing surface. When the ratio becomes larger than .60 (such as in sections near the chine) a rapid increase in the initial spray trajectory angle results. Applying these two-dimensional flow concepts to the three-dimensional planing surface, it is evident that, as plane k-c approaches the chine, two continuous changes in flow patterns result. In the first the spray thickness increases, while in the second the initial spray trajectory angle increases rapidly for sections near the chine (Figure 1, page 30). The large initial spray trajectory angle near the chine can account for the formation of the main spray blister previously described. This flow process indicates that the main spray is generated in a localized area in the region of the stagnation line intersection with the chine. The fact that the spray thickness and initial trajectory angle are large in the area of the chine causes the main spray blister to be a relatively heavy sheet which reaches maximum trajectories high enough to wet seriously and to increase the resistance of many exposed areas of a seaplane. It is this main spray sheet with which the subject report is concerned.

In summary then, the preceding physical descriptions indicate that the whisker spray and main spray are generated by essentially the same physical flow processes. The different shapes of each spray pattern are attributed to the sharp increase in initial trajectory angle (Figure 1) and the continuous increase in elemental spray thickness as the effective two-dimensional flow planes approach the chine. Inasmuch as the pressure (and, consequently, the velocity) changes rapidly near the chine end of the stagnation line, it is not expected that the superposition of the cross-flow and spray-root flow will result in accurate quantitative results. Nevertheless, it does give a qualitative picture of the hydrodynamic flows which lead to the development of whisker and main sprays. In order to explore further the mechanism of main spray generation and to verify the assumption that it is generated in a localized region near the stagnation line intersection with the chine, a few simple experiments were performed. These are described in the following section.

EXPERIMENTAL STUDIES

The experimental investigations performed in this study of planing surface sprays included both broad explorations to define the origin of the spray generation and detailed measurements to relate the main spray geometry with hull and planing parameters.

Exploratory Tests to Determine Origin of Main Spray

Spray Dam Tests

It has been hypothesized in the previous general discussion that a main spray originates virtually from a "point" in the immediate vicinity of the stagnation line intersection with the chine. It was considered important to verify experimentally this hypothesis since *casual observations of a main spray blister on a high speed planing model give the impression that water issues along the entire wetted chine length, thus forming the spray blister.* In order to explore this point a thin sheet-metal strip .20 beams long was mounted vertically at several longitudinal positions along the chine of a 20 degree deadrise planing surface as shown in the following sketch. (The dimensions of the vertical chine strip are defined in this sketch.)

The planing surface was set at a fixed heave and at a fixed trim angle of eight degrees and towed at a constant speed coefficient of 3.00. The resultant spray pattern for these planing conditions is shown in Figure 3a on page 32. As the small vertical chine strip was moved to positions suc-

cessively forward, no effect on the main spray blister was noticed until the strip was placed at the stagnation line intersection with the chine. At this point almost the entire main spray blister was suppressed by the minute spray strip. Figure 3 presents photographs indicating the effectiveness of the small local chine strip in practically eliminating the main spray blister. As evident in these photographs, the chine or spray strip was installed only on the starboard side. The main spray blister on the port side is seen to be essentially identical in both photographs. As the local chine strip was moved ahead of the stagnation line intersection with the chine, the main spray blister was undisturbed but a deflection of the whisker spray in the area of the chine strip took place.

One other hypothesis concerning the origin of a main spray also was explored. It had been suggested that the velocity component along the stagnation line (V_s) might cause a fluid flow in the direction of the chine and that, upon leaving the chine, this fluid jet would expand to develop the main spray blister. In order to investigate this hypothesis a small longitudinal flat projecting plate .20 beams long and .05 beams deep was placed in line with the flow normal to the bottom and across the stagnation line successively at athwartship locations of .25 and .375 beams from the keel. It was intended that this spray strip would obstruct the fluid flow along the stagnation line and, consequently, reduce the fluid volume and alter the geometry of the main spray blister. A sketch of this local spray dam and photographs of its effects on the main spray are given in Figure 4 on page 33. It is evident that the inboard spray dams have only a small effect on altering the appearance of the main spray blister. It is obvious from comparing the photographs in Figures 3 and 4 that the chine spray strip is much more effective than an inboard strip in controlling the main spray blister.

Dye Injection Tests

To characterise further the origin of planing surface sprays and particularly to define the division of the undisturbed water surface into whisker and main spray, a series of observations were made of the steady-state patterns when a blue dye was added to the fluid at various locations

around the planing surface. The dye was carried on the test model and released from a hopper as a continuous, thin liquid stream. The locations at which the dye was introduced onto the free water surface are shown in Figure 5 on page 34. During each test run colored motion pictures were taken to establish the distribution of the dye into the areas of spray and wake. (These films are available at ETT.) An analysis of these test results indicated several qualitative conclusions concerning the basic development of the spray patterns.

The dye was first introduced at position one (intersection of stagnation line with chine) to reestablish the fact that main spray issues from a single small region. As had been expected, the entire main spray blister became colored. When the dye injection was moved forward to position two (in the area of the whisker spray) the main spray was uncolored and streaks of blue appeared in the area of the whisker spray surrounding the point of dye introduction. The blue dye stream then was moved to positions aft of the stagnation line intersection with the chine (positions three and four). In these positions the main spray blister remained uncolored and the blue dye appeared in the wake of the planing surface.

The dye hopper next was moved ahead of the planing surface and the dye was introduced onto the undisturbed level water surface (positions five through ten). In position five occasional streaks of blue appeared in the whisker spray, the main spray remained uncolored and a major portion of the dye appeared as a longitudinal centerline streak in the wake of the planing surface. At position six substantial areas of the whisker spray were colored, but the main spray and wake remained uncolored. When the dye was placed in positions seven, eight and nine, the main spray blister was colored blue, but the whisker spray and wake remained uncolored. When the dye was moved to position ten both the spray and wake remained uncolored and a thin blue streak appeared on the water surface parallel to the centerline of the model.

The qualitative results of this exploratory dye experiment reaffirmed the conviction that the main spray blister originates from a single small region at the stagnation line intersection with the chine and also showed that

(1) the undisturbed fluid ahead of and along the centerline of the model appeared in the wake;

(2) the undisturbed surface fluid ahead of the model and for a distance of approximately .40 beams outboard of the keel appeared in the whisker spray;

(3) the undisturbed free surface fluid lying in a band approximately 0.10 beam on either side of the chine line was generated into the main spray blister;

(4) any free surface fluid further outboard of the keel than 0.70 beams did not contribute to either spray formation.

Detailed Measurements of Main Spray

Test Program and Procedure

Detailed measurements were made of (1) the maximum height of the main spray relative to the undisturbed water surface and (2) the lateral position of the maximum spray height relative to the planing model. The main spray dimensions were determined for simple prismatic deadrise models having a beam of nine inches and deadrise angles of 0, 10, 20 and 30 degrees. The models were tested over a trim angle range $6 \leq \tau \leq 15$ degrees, a speed coefficient range $1.0 \leq C_v \leq 4.0$, and for mean wetted length-beam ratios $\lambda \leq 2.50$. Brief investigations were made on the effect of simple chine spray strips in reducing the height of the main spray blister and on the effect of a wind screen towed ahead of the model.

At the start of this investigation the spray dimensions were obtained by the three-view scheme developed by Locke[7] using a single overhead camera and two mirrors. The details of this technique are described in Reference 7. Early in the investigation it was found that this technique presented difficulties in obtaining a consistent set of data mainly because the whisker spray obscured the main spray in many of the views. Furthermore, the necessary delay in processing the exposed film prevented the establishment of running data plots. To circumvent these difficulties, it was decided to use a Polaroid-Land camera which was set up at the side of Tank No. 3 in order to photograph the side elevation of the model and its asso-

ciated main spray blister. The rapid self-developing film used in this camera provided spray height data immediately after the end of each test run. A 70 mm camera was used simultaneously to photograph a rear view of the main spray in order to provide data on the lateral position of the spray blister. A grid board was attached to the side of the model and was used along with the Polaroid camera to measure the side elevation dimensions of the main spray blister. Proper corrections were made to the readings to account for the difference in the height between the top of the spray and the center of the Polaroid camera. A suitable static calibration was provided for the 70 mm camera.

Appearance and Behavior of Main Spray in Model Scale

Prior to presenting the results of the detailed spray measurements, a description will be given of the general appearance and behavior of the main spray during the model tests. This will serve as background for interpreting the measured results.

The series of side-view photographs given in Figure 6 on page 35 illustrates a typical variation in the appearance of the main spray as the speed of the model was increased. Figure 7 on page 36 presents the corresponding stern view photographs of the same test runs. These photographs are copies of the actual pictures used to establish the main spray height and lateral positions. In these pictures the test model is a 20-degree deadrise, nine-inch beam prismatic surface planing at a trim angle of 12 degrees. No main spray formation is evident for $C_v < 1.50$. Instead a small pile-up of water is visible in the area of the chine intersection with the water surface. At low speed coefficients the stern views clearly show the small bow wave formation attached to the model. At $C_v = 1.50$ the typical main spray blister appears as a thin continuous sheet of fluid. At $C_v = 2.00$ the main spray blister becomes higher and larger but still maintains its essentially continuous appearance. When the C_v is increased to 2.50 the spray sheet increases in height and develops an instability which is characterized by the appearance of sinusoidal oscillations (not unlike that of a flag in a breeze). This instability is similar to that described by Dundurs and Hamilton[8] in their basic study of the stability of thin sheets.

At $C_v = 3.00$ the main spray instability attains oscillations severe enough to rupture areas of the spray sheet and to form droplets of water which are thrown away from the main spray sheet. When the planing speed is increased to $C_v = 3.50$, the general appearance of the main spray is no longer that of a continuous blister but, for the most part, consists of broken, dense droplets of fluid whose trajectory is a continuation of that portion of the main spray sheet which is still intact. This characteristic is most clearly illustrated in the stern view photographs of Figure 7 on page 36. Figure 7 also shows that the effect of increasing the speed coefficient causes the inboard surface of the main spray sheet to move closer to the chine of the planing model and, eventually to obscure the bow wave formation which had developed at low speeds.

The thin, continuous "glassy" appearance of the main spray sheet at moderate values of C_v is characteristic of the main spray developed during the model tests. Prototype main spray formations usually are broken, dense droplets of water which present an overall milky white appearance. Because of the continuity and small radius of curvature of the model main spray sheet, surface tension forces are large, relative to the inertia forces. Consequently, these forces have a strong effect in keeping the spray blister intact. This curved spray sheet acts as a highly cambered airfoil which develops an aerodynamic lift caused by the action of the relative wind stream into which the spray sheet is thrown. The lift force then raises the spray blister to a somewhat greater height than it would achieve if the model were towed in a vacuum.

This lifting effect was noted in a brief experimental investigation which was made with a 30 degree deadrise model towed at trim angles of 12 and 15 degrees, with and without a deflecting windscreen installed ahead of the planing model. For the nine-inch beam model at a $C_v = 2.00$, the main spray height without a windscreen was approximately 20 percent higher than that with a windscreen. It was also found that, without a windscreen, the spray sheet became unstable at a lower C_v and that its instabilities were more pronounced than with a windscreen. At higher C_v when the spray sheet was broken up into dense droplets of water, the windscreen had little effect on the spray appearance. Because of the brief, exploratory nature of

the windscreen investigation a thorough evaluation of the effect of surface tension and aerodynamic forces on model spray geometry at small velocity coefficients was not possible. However, it can be hypothesized that, as the model size is increased, the inertia forces will become much larger than the surface tension forces and, consequently, the extent of the main spray which remains intact shrinks. In the prototype, the sheet-like behavior usually is confined to the first few feet of the spray and beyond that region the spray disintegrates into myriad droplets which appear to continue upward and outward on the initial trajectory of the spray sheet. Because of the unknown magnitude and consequences of surface tension and aerodynamic forces in model tests of main spray, a more comprehensive and basic study of these effects is recommended, particularly for very small model sizes.

The correlation between model and corresponding prototype spray heights has been the subject of several papers (References 7, 9, 10 and 11). The results of these studies have been inconclusive. Some indicate good agreement between model and prototype spray heights, while others indicate the prototype spray to be somewhat higher than the model spray. One of the difficulties in such a comparison has been the unreliability of the prototype data. Sufficiently accurate measurements of the prototype trim, heave, draft and spray height have not been available to make accurate comparisons with model results. Furthermore, prototype tests are always in a power-on condition where propeller slipstream velocities may influence the spray height. One uniform recommendation made by most investigators is that further study of the characteristics and behavior of model and prototype spray formations is highly desirable.

In order to eliminate the aerodynamic effects on model spray blisters it was decided to measure all spray heights with the model running behind a windscreen. It was believed that the resultant spray heights would be more like those of the broken prototype spray which appeared to be uneffected by the free stream velocity.

As further illustration of the spray appearance with varying planing parameters, Figure 8 on page 37 has been prepared to illustrate the spray variation with trim angles and Figure 9 on page 38 has been prepared to

show the variation with deadrise angles. Both series of photographs are for a nine-inch beam model planing at $C_v = 2.00$. It is evident that the "glassy", continuous appearance of the main spray is maintained for trim angles from six to 15 degrees. Figure 9 shows that at $\beta = 0$ degrees the main spray does not exhibit the usual blister appearance but rather appears as a longitudinal plume of water. For $\beta = 10$, 20 and 30 degrees, the blister appearance of the main spray again is evident. The subsequent section of this report will define quantitatively the variation in spray geometry with deadrise, trim and velocity coefficient.

Height of Main Spray from Model Tests

The maximum heights, ζ, of the main spray blister, as measured from the Polaroid-Land pictures, are plotted in Figure 10 on page 39 for the four tested deadrise surfaces. All test data were obtained for the nine-inch beam models planing at a fixed $\lambda = 2.50$ and towed behind a windscreen. The height, ζ, is the distance between the level water surface and the maximum height of the spray blister which remains intact. At values of C_v where the spray broke into rather large droplets, an accurate determination of the maximum spray height was not possible.

In Figure 10, the ratio $\zeta / V^2/2g$ is plotted against C_v for each test trim angle and deadrise model. This normalized representation of the spray height was used in order to establish whether or not the spray followed a ballistic trajectory upon leaving the chine of the planing model. Examining the data for each deadrise it can be seen that, beyond a C_v of approximately 1.50, the ratio $\zeta / V^2/2g$ is a constant for a given trim angle, thus, indicating that the spray height varies as the square of the speed for a given combination of planing conditions. For $C_v < 1.50$ it is seen that, with decreasing speed, the spray height decreases much more rapidly than the square of the speed. This is attributed to the fact that, in this speed range, the basic flow pattern about the model is influenced strongly by gravity* and to some extent by surface tension. For 10, 20

---

*This is not to be confused with the influence of buoyancy whose effect is apparent in planing lift coefficient up to a C_v of about 10.

and 30 degrees deadrise surfaces a limiting line is drawn to indicate the combinations of C_v and τ at which the spray blister breaks up into large droplets.

Although it was difficult to measure accurately the maximum spray height during the spray break-up, it was expected that, since the main spray development followed a ballistic trajectory, the maximum height of the water droplets at high C_v could be defined by the normalized coefficients $\zeta/V^2/2g$. It is interesting to note that, for a given trim, the spray sheet remained intact at higher speeds as the deadrise angle was increased from 10 to 30 degrees. Observations of the model spray patterns indicated that, with increasing deadrise, the spray blister became narrower in width and was directed further aft. The narrower width would make the spray blister more stable and, consequently, would delay the development of instabilities in the sheet.

For $\beta = 0$ degrees, no spray break-up limit line is shown in Figure 10 (page 39). It should be recalled from the discussions on page 21 that the usual spray blister was not developed for $\beta = 0$ degrees, but rather the spray appeared as a long longitudinal plume of water running close to the chine of the model. In order to investigate the effect of λ on the main spray height, several test runs were made with each deadrise model set at $\lambda = 0.80$ and 1.50. For this test range of λ, no discernable effect of mean wetted length-beam ratio on the spray geometry was evidenced. This follows from the fact that the main spray generation was dependent solely on the local conditions at the stagnation line intersection with the chine.

The limiting values of the ratio $\zeta/V^2/2g$ for each trim and deadrise combination have been taken from Figure 10 and replotted in Figure 11 on page 40 in order to show more clearly the effect of trim and deadrise on main spray height. It is seen that, at a given trim angle, the spray height is smallest for $\beta = 0$ degrees, increases to a maximum value when β is approximately 10 degrees, and then decreases as β is increased to 30 degrees. Increasing τ at any given β causes a large, almost linear increase in maximum spray height. It is evident from Figure 11 that, on the whole, the main spray height is much more sensitive to trim angle changes than to changes in deadrise angle.

Superposed on the plots of Figure 11 are lines of the constant stagnation line pressure coefficient, $p_s/\frac{1}{2}\rho V^2$. The combinations of τ and β which develop a constant p_s were obtained from Figure 15 of Reference 6 which shows that the stagnation line pressures are solely dependent upon the angle between the stagnation line and keel, measured in the plane of the bottom. Consequently, for given values of stagnation pressure coefficient and trim angle, there is a corresponding deadrise angle which will develop this pressure. It is interesting to note from Figure 11, that the maximum main spray heights are not strongly dependent upon the stagnation pressure. Instead, for a given stagnation pressure, there is a linear increase in spray height with increasing deadrise angle. Similarly, by a cross-plot of Figure 11 using the trim angle as an abscissa, it can be shown that, for a given stagnation pressure, a linear increase of spray height takes place as the trim angle is increased. Both increases follow from the fact that, for constant p_s, an increase in trim or deadrise results in larger effective angles of attack of the two-dimensional flow plane used to describe qualitatively the main spray generation (page 12). It will be recalled that the angle of attack of the two-dimensional flow plane is the angle between the line of intersection of a plane normal to the bottom and perpendicular to the stagnation line and the line of intersection of this plane with the level water surface. The value of this angle in terms of trim and deadrise is given in Figure 3 of Reference 12. The angles of attack of the effective two-dimension planes were calculated for the trim and deadrise combinations which developed the constant ratios $p_s/\frac{1}{2}\rho V^2$ shown in Figure 11. Although these results are not tabulated in this report, it was found that the initial trajectory angles corresponding to the maximum measured spray heights were always larger than the effective angle of attack of the two-dimensional planes. This fact further indicates that there is a large turn-up of the basic fluid flow as it leaves the chine -- such as was associated with Green's flow which was described on page 7 and in Reference 2. It is again emphasized that the descriptions of main spray generation contained herein give a qualitative picture of the mechanism, but a detailed three-dimensional study is necessary of the flow in the region of the stagnation line intersection with the chine in order to describe quantitatively the main spray geometry.

Lateral Position of Maximum Spray Height from Model Tests

The transverse position, η , of the maximum height of the main spray blister measured outboard of the chine is shown in Figure 12 (page 41) for the four test models. For each deadrise model, the coefficient $\eta/V^2/2g$ is plotted against C_v for each test trim angle.

For deadrise angles of zero and 10 degrees, it is evident that the ratio $\eta/V^2/2g$ is essentially constant for each test trim angle when C_v is larger than approximately 2.00. For β = 20 degrees a slight reduction in the ratio $\eta/V^2/2g$ is noted when C_v is increased to values larger than 2.00. For β = 30 degrees, the ratio $\eta/V^2/2g$ is constant for the range $2.00 \leq C_v \leq 3.50$ and then decreases as C_v is increased to values larger than 3.50. If the ballistic concept of main spray generation is applied, it becomes apparent that the athwartship component of the spray trajectory angle is a function of the speed coefficient for each deadrise angle. It should be recalled from the discussions of spray height (page 21) that the spray height varied as the square of the speed for all test $C_v \geq 1.50$, thus indicating that the trajectory angle relative to the horizontal is independent of C_v. From the data in Figure 12 on page 41 it appears that, for a given trim and deadrise angle, the athwartship component of the trajectory angle first increases with C_v, then remains constant over a small increment of C_v and finally is reduced as C_v is further increased. No attempt has been made in this analysis to evaluate this athwartship angle for the various test combinations of τ, β and C_v. However, it is clear from Figure 12 that the absolute distance, η , increases constantly with C_v over the test speed range.

In order to isolate the effect of τ and β on the lateral position of the maximum spray height, the maximum values of the ratio $\eta/V^2/2g$, for a given τ and β combination, have been taken from Figure 12 and replotted on Figure 13 on page 42. It is clear that, for all test deadrise models, the lateral position of the maximum spray height increases with increasing trim angle. The effect of increasing deadrise from zero to 20 degrees, for a given trim angle, is to increase the lateral position of the spray blister. When the deadrise is increased to 30 degrees the lateral

position is decreased. The minimum lateral position of the main spray occurs at a deadrise angle of zero degrees for all test trim angles.

Effectiveness of Chine Flare in Controlling Main Spray Height

A brief investigation was made of the effect of simple vertical and horizontal chine strips in altering the height of the main spray blister. For this investigation the nine-inch beam, 20-degree deadrise model was tested at trim angles of 8, 12 and 15 degrees over a C_v range from approximately 1.50 to 4.00. Several vertical and horizontal chine flares were investigated at each combination of planing parameters.

The vertical chine strip was a .064-inch dural plate which was fastened to the side of the model along the entire length of the starboard chine. The bottom edge of the vertical chine plate was set at depths of .006 b, .011 b, .022 b and .056 b below the chine line. Polaroid-Land pictures were taken of the resultant spray pattern in order to establish the maximum heights of the main spray blister. The results of this investigation are presented in Figure 14 (page 43) which shows that the vertical spray strip is extremely effective in reducing the height of the main spray. For a vertical chine strip 5.6 percent of the beam deep, the spray height was reduced to approximately 65 percent of the height developed in tests of the model without chine strips.

At trim angles of eight and 12 degrees the figure shows that increasing the depth of the vertical spray strips to .011 b causes significant reductions in the spray height. Further increases in the depth of the spray strip result in only moderate reductions in spray height. It appears that, for these trim angles, little gain in spray reduction will be achieved by using vertical spray strip depths larger than 5.5 percent of the beam. These results are in excellent agreement with conclusions reached by Locke[13]. At test trim angles of 15 degrees, a continuous reduction in spray height appears as the depth of vertical strip is increased. No attempt was made to establish the limiting depth at which the effectiveness of vertical spray strips was reduced.

The horizontal chine strip used in these tests was formed by filling the area between the bottom edge of the vertical chine strip and the bottom of the model with plasticene. The lower surface of the plasticene fill was horizontal, was faired into the bottom of the model, and was set at depths of .022 b and .056 b below the chine of the model. The results of these tests are plotted in Figure 15 on page 44. It is seen that horizontal chine flare has no effect in reducing the height of the main spray. In fact, at the test trim of 15 degrees, the horizontal chine flare actually caused an increase in spray height as compared to the model without a chine flare. Again, these results confirm the results obtained by Locke in Figure 9 of Reference 13.

Due to structural design difficulties, the vertical chine strip may not be a practical configuration. The introduction of a chine fillet with down flare should overcome this structural difficulty and produce good spray control. It appears to be important in chine flare design to make certain that the edge flows are deflected downward upon leaving the model. In Figure 13 of Reference 13, Locke showed that a down flare angle of 45 degrees is almost as effective as a vertical chine strip.

CONCLUSIONS

Analytical and experimental studies of the main spray associated with prismatic planing surfaces have led to the following conclusions regarding the basic mechanism of its generation and the dependence of its geometric form upon the fundamental planing parameters.

1. The main spray originates from a localized area at the intersection of the stagnation and chine lines.

2. The entire main spray blister can be suppressed effectively by a small local vertical spray dam placed at the stagnation line intersection with the chine.

3. The trajectory angle between the main spray sheet and the horizontal plane is much larger than the trim angle or the angle of the stagnation line above the horizontal. It is the trajectory angle which accounts for the large heights achieved by the main spray blister.

4. The generation of the so-called "whisker" spray at the wetted leading edge of a planing surface is similar to Wagner's semi-infinite two-dimensional type of flow, while the generation of the main spray blister immediately behind the whisker spray is similar to Green's finite-leading-edge (two-dimensional) type of flow. A natural transition from the Wagner-type to the Green-type flow exists at the forward edge of the planing area.

5. The water in the main spray originates from a surface strip of the undisturbed fluid lying ahead of and parallel to the chine of the planing surface for a width approximately .10 beams on each side of the chine line. The surface fluid inboard of this strip appears as a whisker spray, while the fluid outboard of the strip remains on the surface wave generated by the planing surface.

6. Detailed measurements indicate the spray heights vary with the square of the speed for $C_v \geq 1.50$ and depend only on the local flow conditions at the stagnation line intersection with the chine, i.e., do not vary with aspect ratio.

7. The trim angle has a strong effect on the maximum height of the main spray. Spray heights increase approximately linearly with the increasing trim angle.

8. The deadrise angle has only a moderate effect on the maximum height of the main spray. The spray height increases as the deadrise angle is increased from zero to 10 degrees and then decreases as the angle increases above 10 degrees.

9. Vertical chine strips are a very effective means for reducing the spray height. Chine strip depths as small as 2.2 percent of the beam reduce the main spray height almost 65 percent.

10. Horizontally faired chine strips are ineffective in reducing the spray heights.

11. Because of the intact, "glassy" continuous blister which is characteristic of model spray, surface tension forces act through the sheet and the entire sheet is subjected to aerodynamic lifting forces as

it passes through the relative wind stream. The combined effect of these forces on model spray heights should be further investigated.

REFERENCES

1. Wagner, Herbert: "Über Stoss-und Gleitoorgauge an der Oberflache von Flüssiglseiten", Z.f.a.M.M., Bd. 12, Heft 4, August 1932.

2. Green, A.E.: "The Gliding of a Plate on a Stream of Finite Depth", Jesus College. Proceedings of the Cambridge Philosophical Society, Volume 31, October 1935.

3. Pierson, John D., Leshnover, Samuel: "An Analysis of the Fluid Flow in the Spray Root and Wake Regions of Flat Planing Surfaces", Stevens Institute of Technology, Experimental Towing Tank Report No. 335, October 1948. Sherman M. Fairchild Publication Fund Paper No. 166. Institute of the Aeronautical Sciences, New York.

4. Savitsky, Daniel, Neidinger, Joseph W.: "Wetted Area and Center of Pressure of Planing Surfaces at Very Low Speed Coefficients", Stevens Institute of Technology, Experimental Towing Tank Report No. 493, July 1954. Sherman M. Fairchild Publication Fund Paper No. FF-11, Institute of the Aeronautical Sciences, New York.

5. Smiley, Robert F.: "A Semiempirical Procedure for Computing the Water-Pressure Distribution on Flat and V-Bottom Prismatic Surfaces during Impact or Planing", NACA TN 2583, December 1951.

6. Pierson, John D., Leshnover, Samuel: "A Study of the Flow, Pressures and Loads Pertaining to Prismatic Vee-Planing Surfaces", Stevens Institute of Technology, Experimental Towing Tank Report No. 382, May 1950. Sherman M. Fairchild Publication Fund Paper No. FF-2. Institute of the Aeronautical Sciences, New York.

7. Locke, F.W.S., Jr., and Bolt, Helen L.: "A Method for Making Quantitative Studies of the Main Spray Characteristics of Flying-Boat Hull Models", NACA ARR No. 3R11, 1943.

8. Dundurs, J., Hamilton, W.S.: "Disintegration of Seaplane Spray and Flat Sheets", Hydraulic Laboratory, Northwestern University, Evanston, Illinois, June 1955.

9. Locke, F.W.S., Jr.: "An Analysis of the Main Spray Characteristics of Some Full Size Multi-Engine Flying Boats", NACA TN No. 1091, July 1946.

10. Brown, P. Ward: "The Main Spray Characteristics of Flying Boats", Short Brothers and Harland Limited, Hydrodynamics Note No. 41, May 1951.

11. Hugli, W.C., Jr. and Axt, W.C.: "A Comparison of the Main Spray from Models of the XPBB-1, PBM-1 and PBM-3 Flying Boat Hulls with that from the Full Size Flying Boats", Stevens Institute of Technology, Experimental Towing Tank Report No. 297, April 1946.

12. Pierson, John D.; Dingee, David A. and Neidinger, Joseph W.: "A Hydrodynamic Study of the Chines Dry Planing Body", Stevens Institute of Technology, Experimental Towing Tank Report No. 492, May 1954. Sherman M. Fairchild Publication Fund Paper No. FF-9. Institute of the Aeronautical Sciences, New York.

13. Locke, F.W.S., Jr.: "The Effect of Chine Flare on the Spray Characteristics of a Model of the JRF-5", Navy Department, Bureau of Aeronautics, Research Division Report No. DR-1842, November 1956.

FIGURE 1

VARIATION OF SPRAY ANGLE WITH DEPTH OF SUBMERGENCE FOR A TWO-DIMENSIONAL FLAT PLATE AT $\tau = 30°$ (GREEN'S SOLUTION, REFERENCE 2)

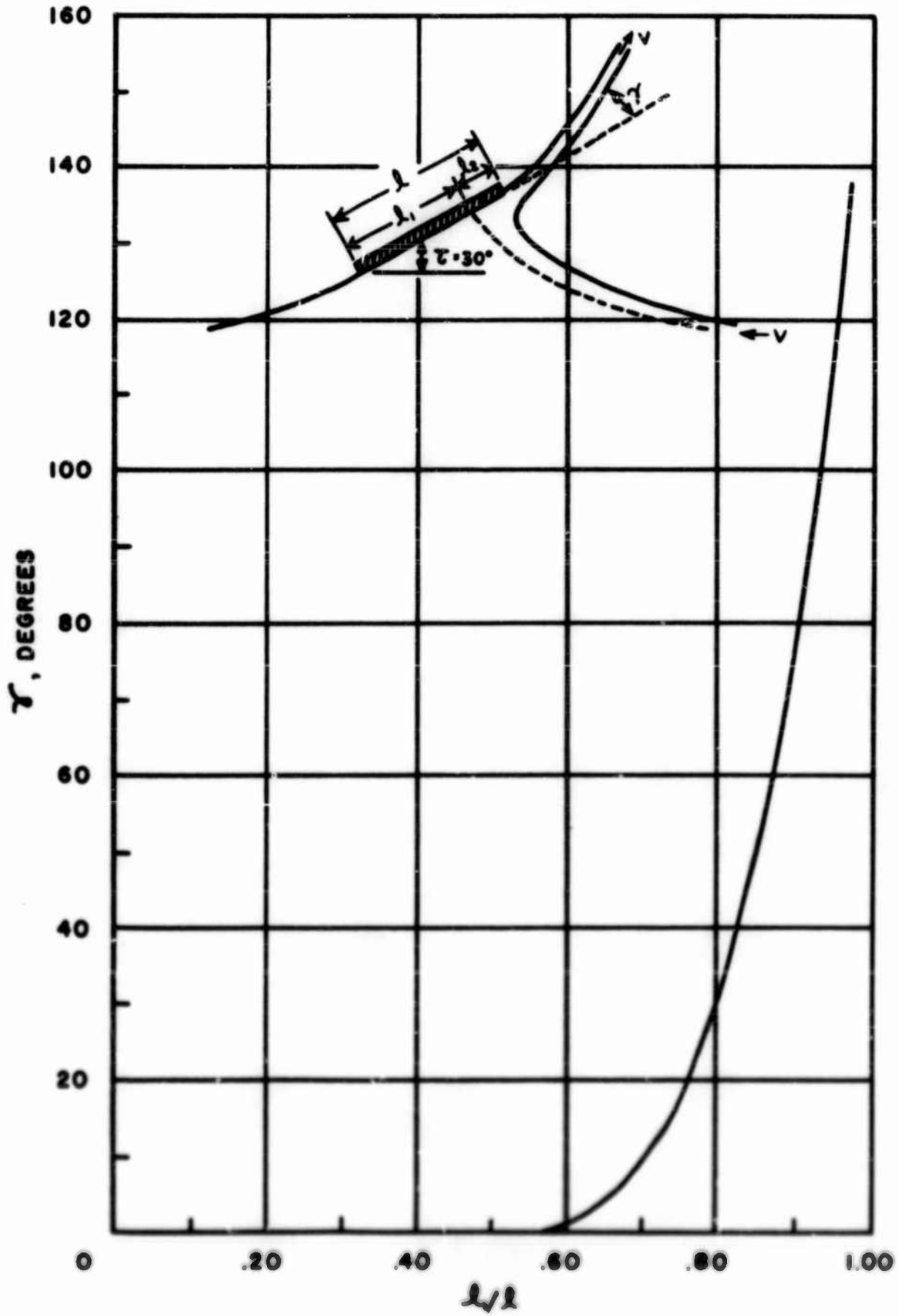

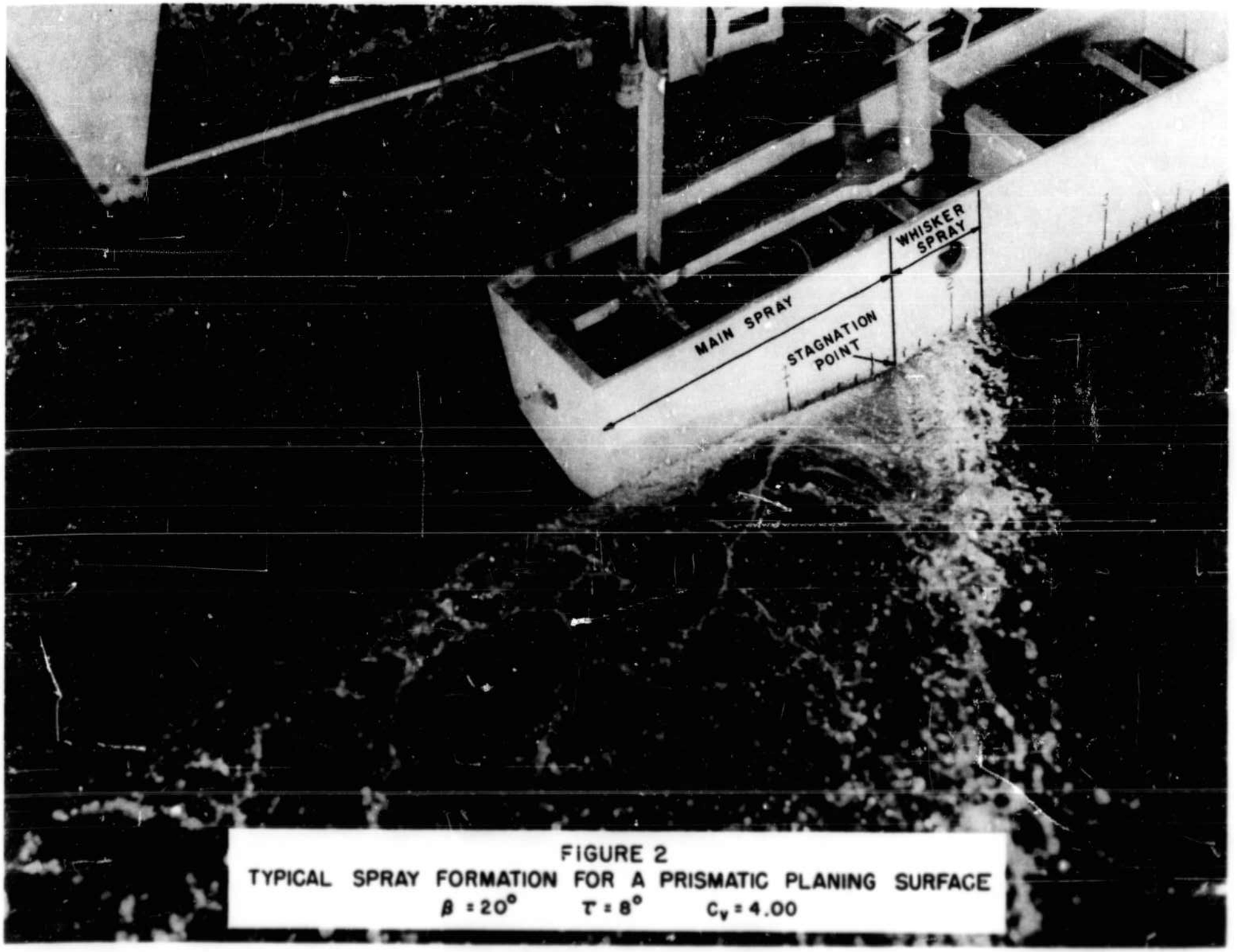

FIGURE 2
TYPICAL SPRAY FORMATION FOR A PRISMATIC PLANING SURFACE
$\beta = 20^\circ$ $\tau = 8^\circ$ $C_v = 4.00$

FIGURE 3
EFFECT ON MAIN SPRAY PATTERN OF LOCAL VERTICAL CHINE STRIP PLACED AT THE STAGNATION LINE INTERSECTION WITH THE CHINE

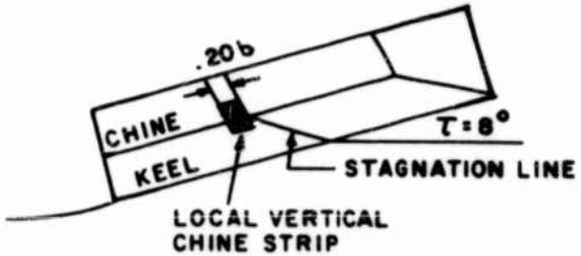

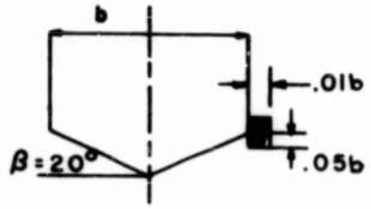

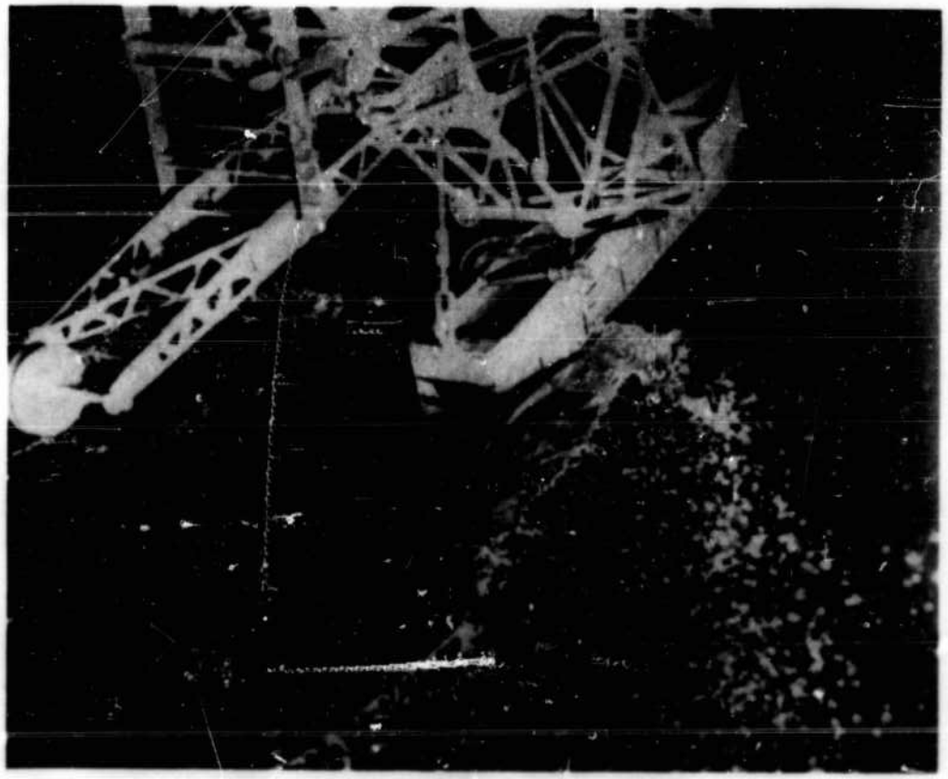

(a) NO LOCAL VERTICAL CHINE STRIP
C_V = 3.00

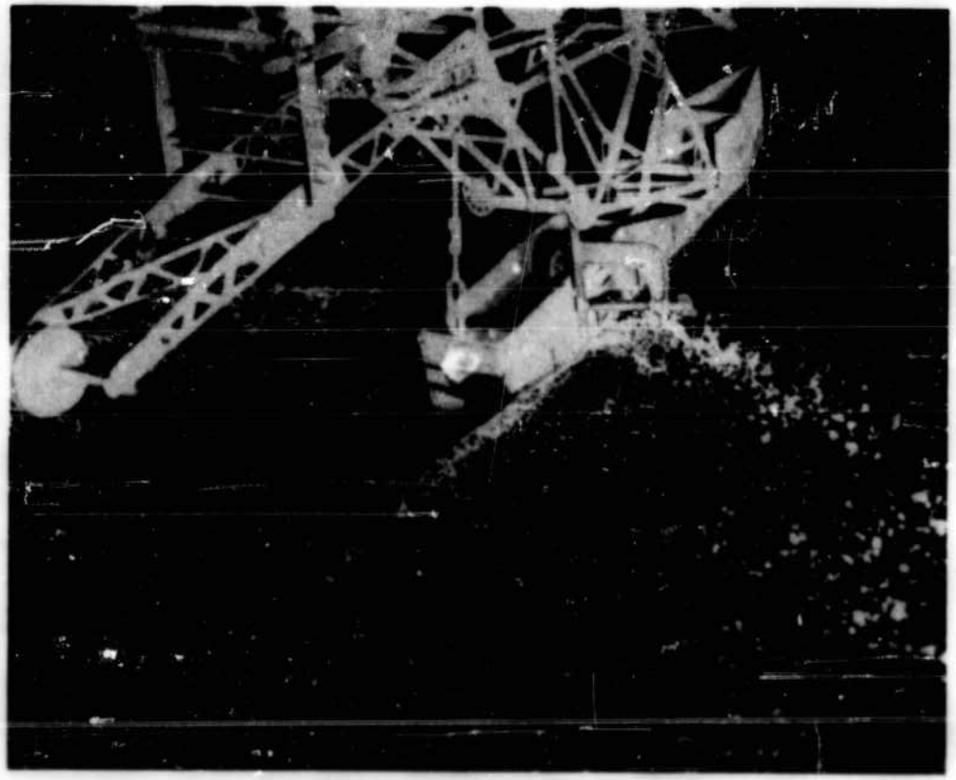

(b) SMALL LOCAL VERTICAL CHINE STRIP PLACED AT THE STAGNATION LINE INTERSECTION WITH THE CHINE
C_V = 3.00

FIGURE 4
EFFECT ON MAIN SPRAY PATTERN
OF LOCAL SPRAY DAMS PLACED NORMAL
TO THE BOTTOM AND ACROSS THE STAGNATION LINE

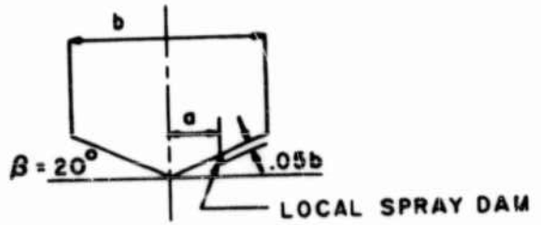

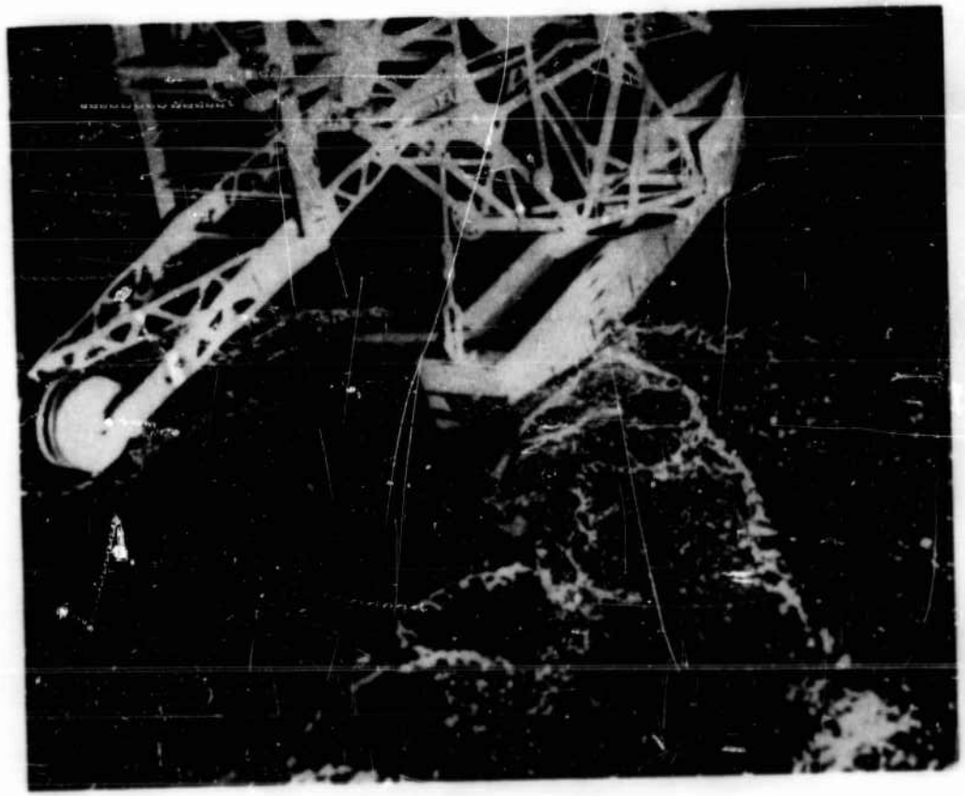

(a) LOCAL SPRAY DAM AT a=b/4
C_v = 3.00

(b) LOCAL SPRAY DAM AT a = b/8
C_v = 3.00

FIGURE 5
LOCATION OF BLUE DYE POSITIONS
($\beta = 20°$, $b = 5''$, $C_v = 3.00$)

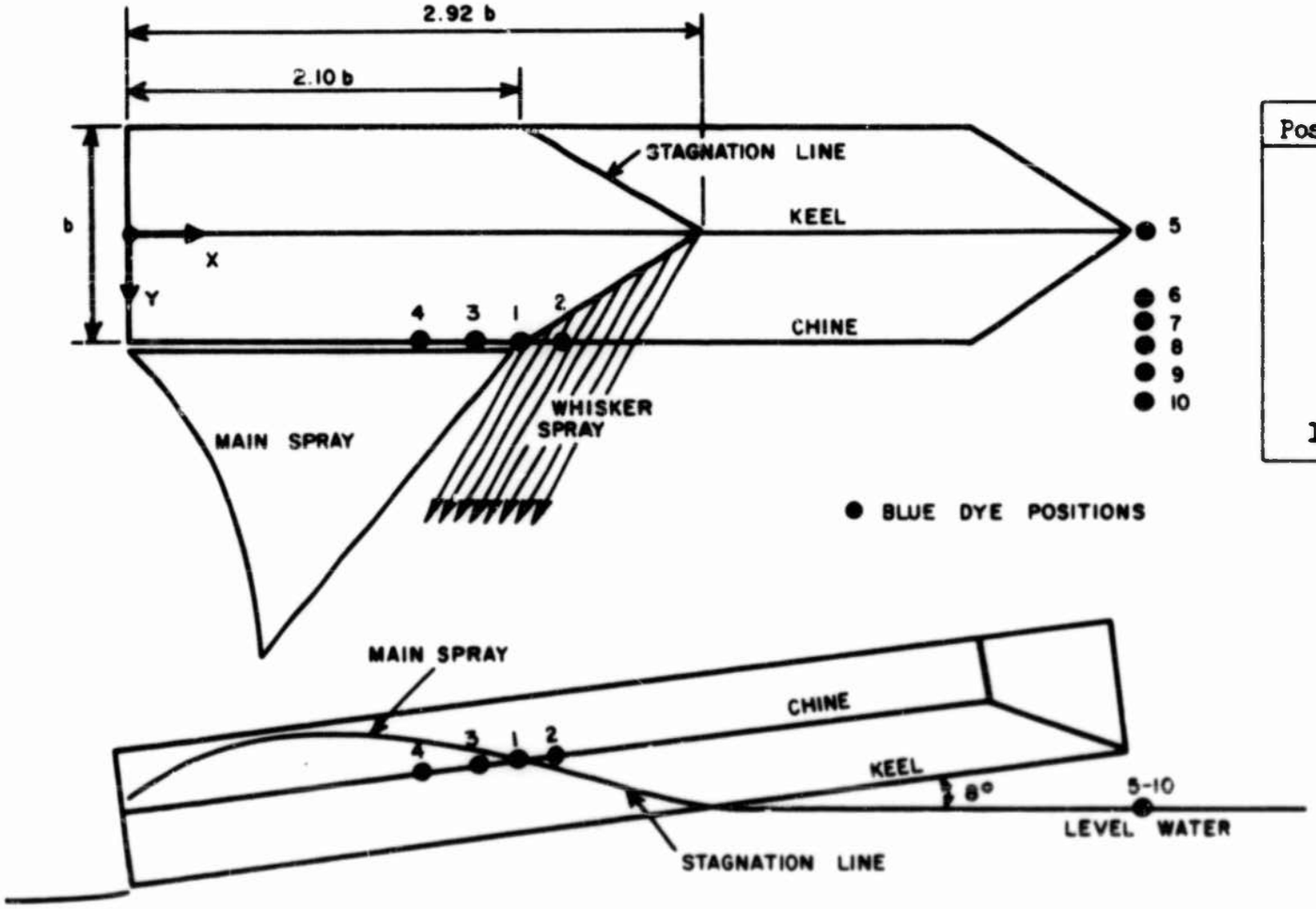

Position	x	y
1	2.10 b	.50 b
2	2.20	.50
3	2.00	.50
4	1.50	.50
5	7.80	0
6	7.80	.24
7	7.80	.38
8	7.80	.50
9	7.80	.60
10	7.80	.68

FIGURE 6
VARIATION OF MAIN SPRAY PATTERN
WITH INCREASING SPEED COEFFICIENT
(SIDE VIEW)
$\beta = 20°$ $\tau = 12°$ $b = 9"$

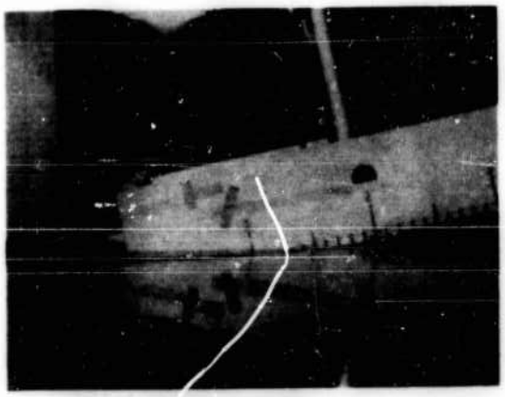

$C_v = 0.64$

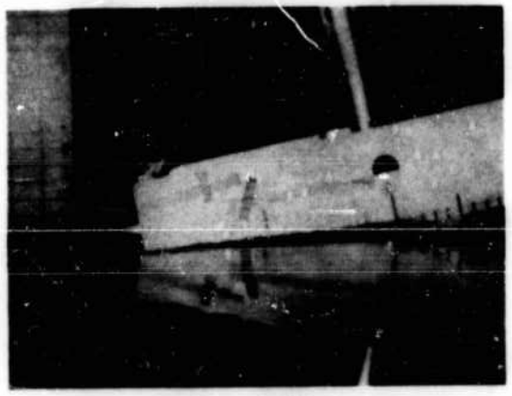

$C_v = 1.00$

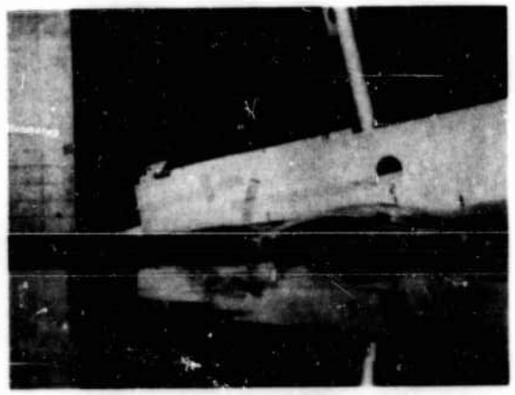

$C_v = 1.50$

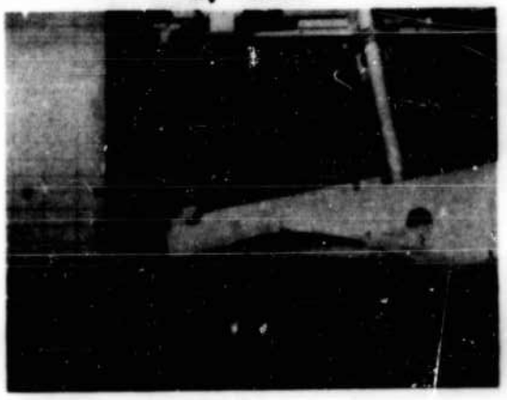

$C_v = 2.00$

$C_v = 2.50$

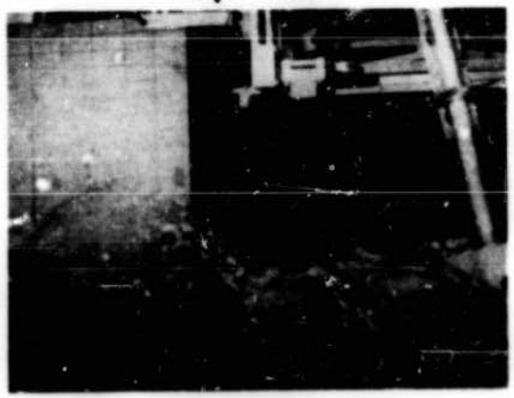

$C_v = 3.00$

$C_v = 3.50$

FIGURE 7
VARIATION OF MAIN SPRAY PATTERN
WITH INCREASING SPEED COEFFICIENT
(STERN VIEW)
$\beta = 20°$ $\tau = 12°$ $b = 9"$

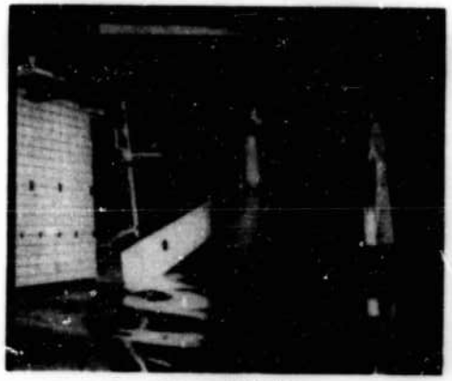

$C_V = 0.64$

$C_V = 1.00$

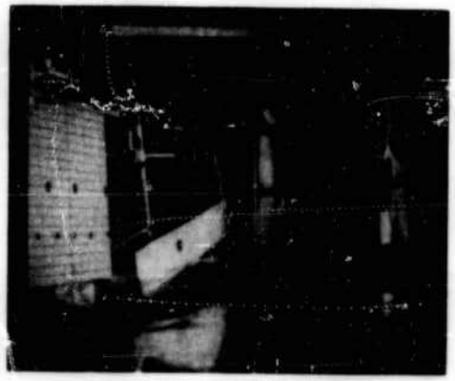

$C_V = 1.50$

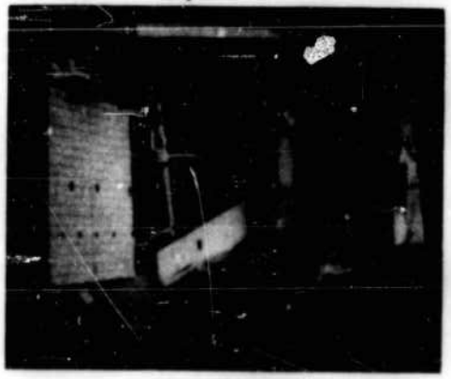

$C_V = 2.00$

$C_V = 2.50$

$C_V = 3.00$

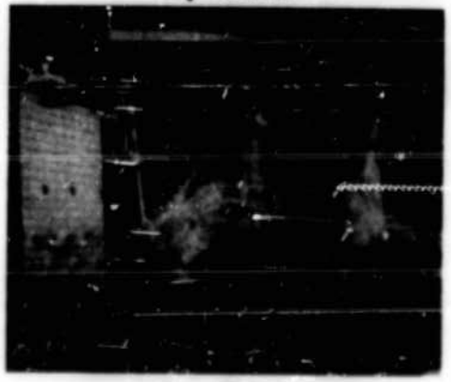

$C_V = 3.50$

FIGURE 8
VARIATION OF MAIN SPRAY PATTERN
WITH INCREASING TRIM ANGLE
(SIDE VIEW)
$\beta = 20°$ $C_V = 2.00$ $b = 9"$

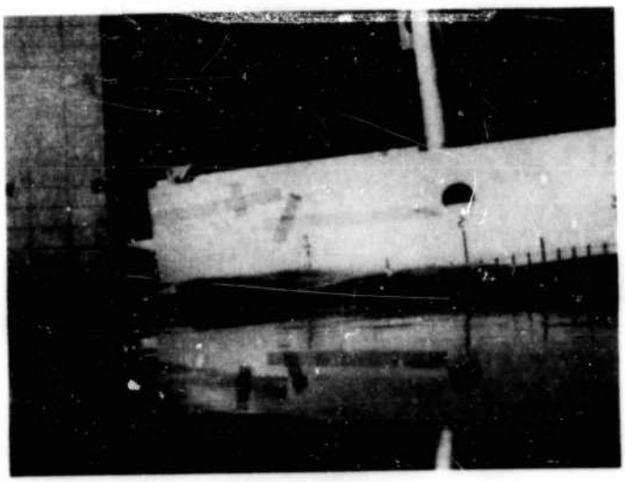

$\tau = 6°$

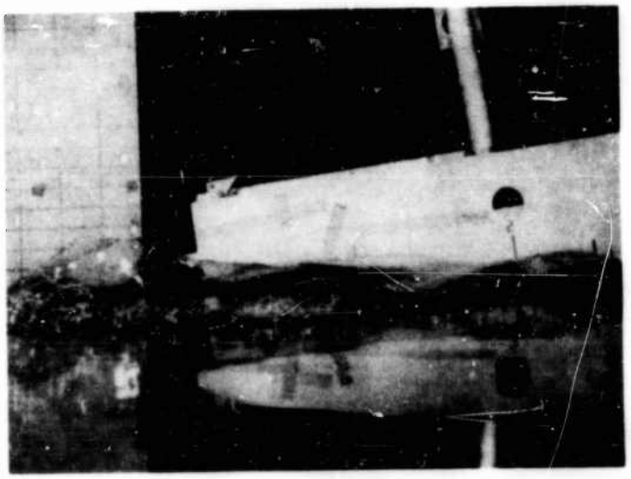

$\tau = 8°$

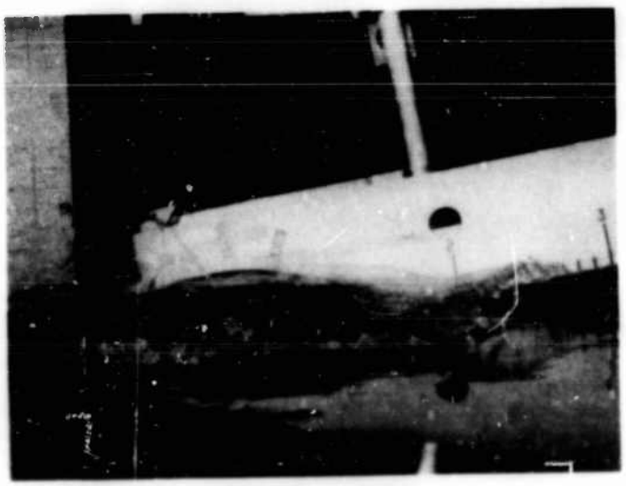

$\tau = 9.5°$

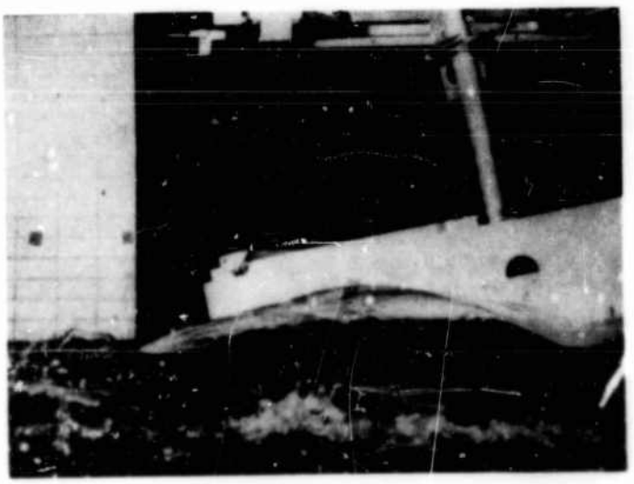

$\tau = 12°$

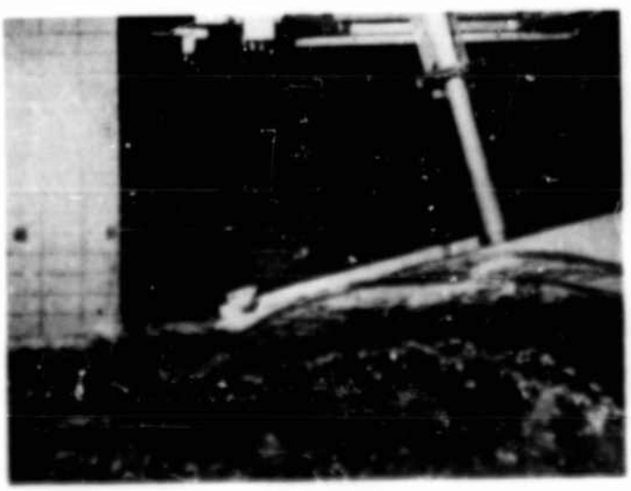

$\tau = 15°$

FIGURE 9
VARIATION OF MAIN SPRAY PATTERN
WITH INCREASING DEADRISE ANGLE

$\tau = 12°$ $C_V = 2.00$ $b = 9''$

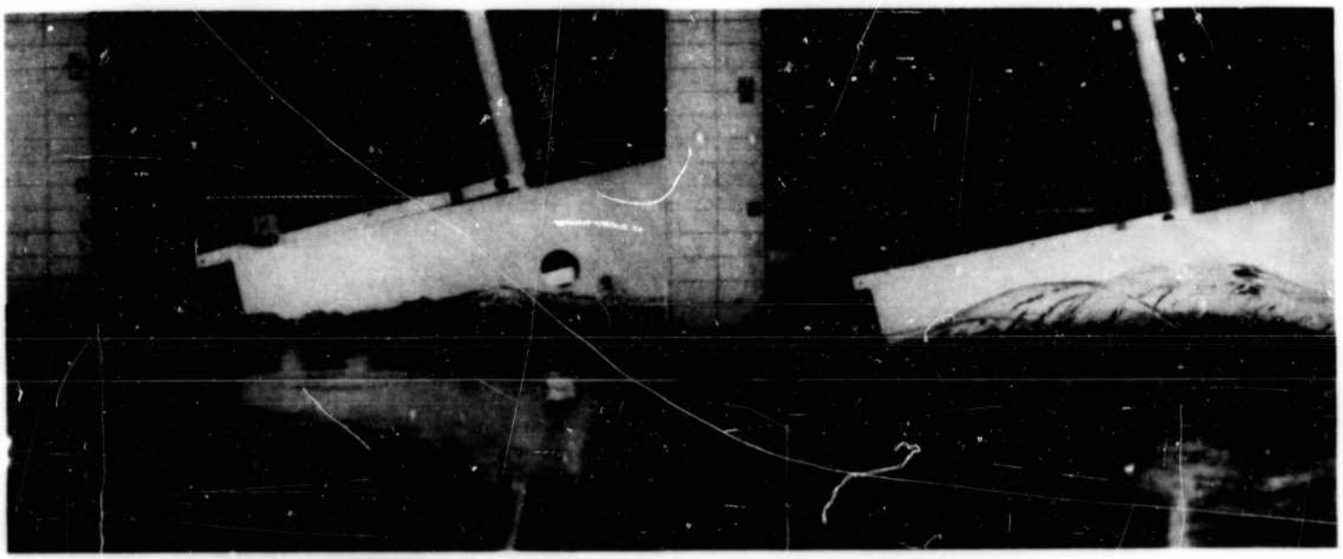

$\beta = 0°$ $\beta = 10°$

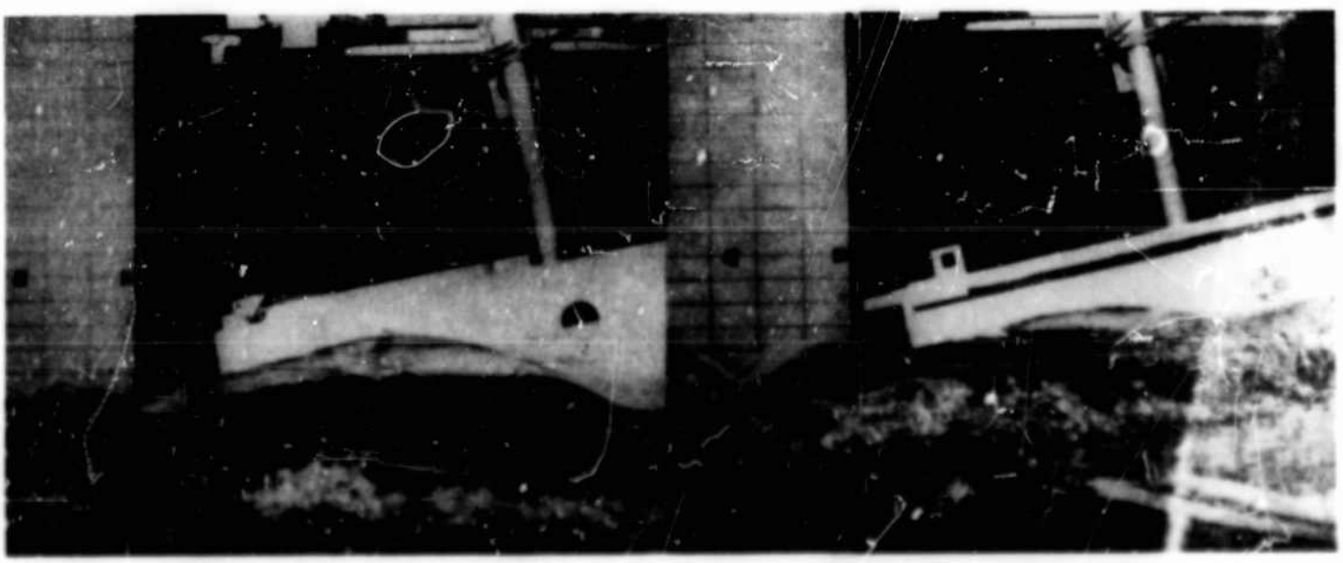

$\beta = 20°$ $\beta = 30°$

FIGURE 10

VARIATION OF MAXIMUM HEIGHT OF MAIN SPRAY BLISTER WITH SPEED COEFFICIENT AND TRIM ANGLE

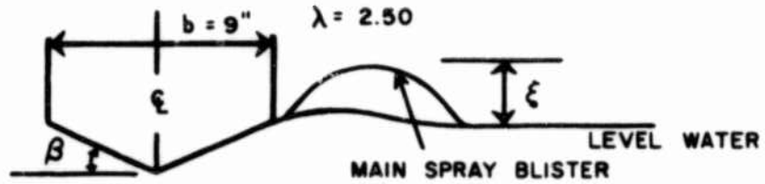

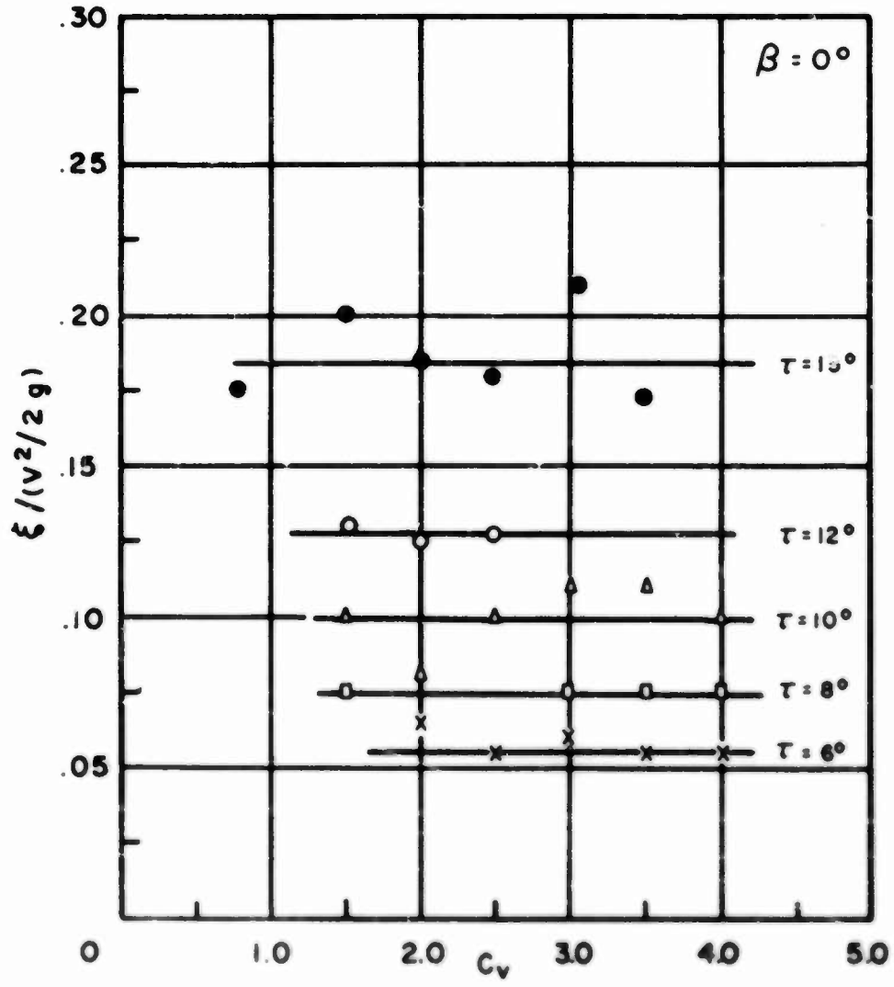

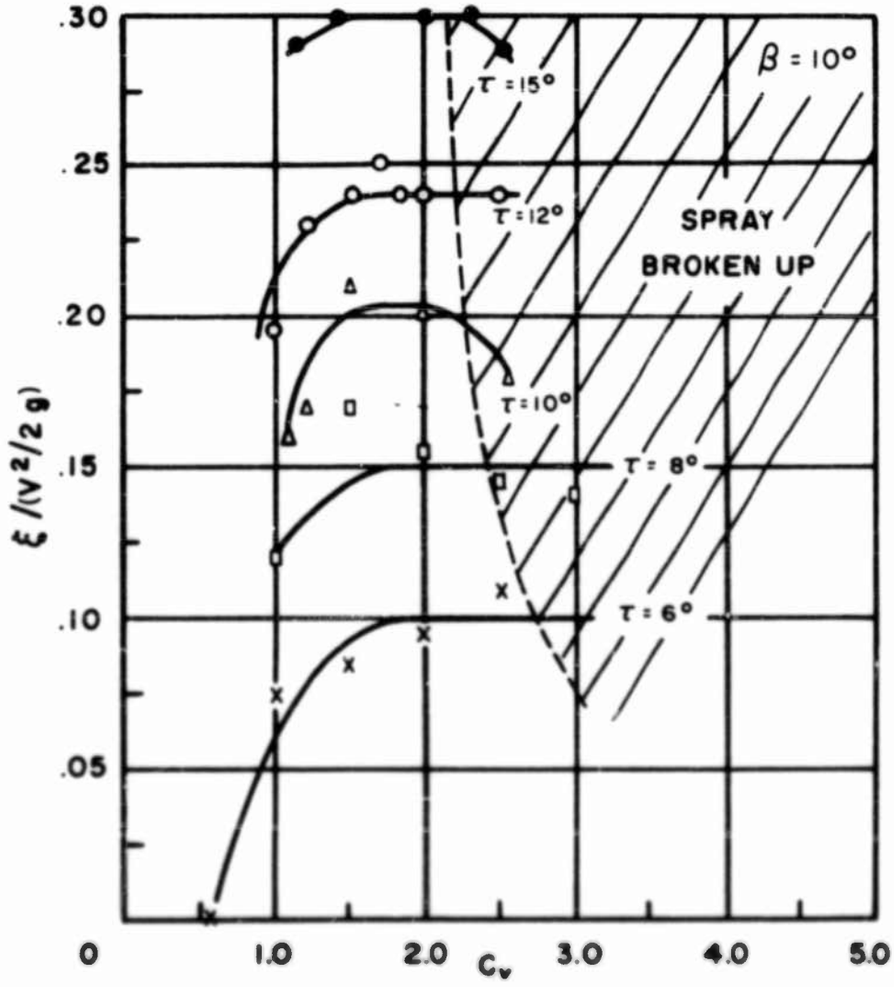

FIGURE 10
(CONTINUED)

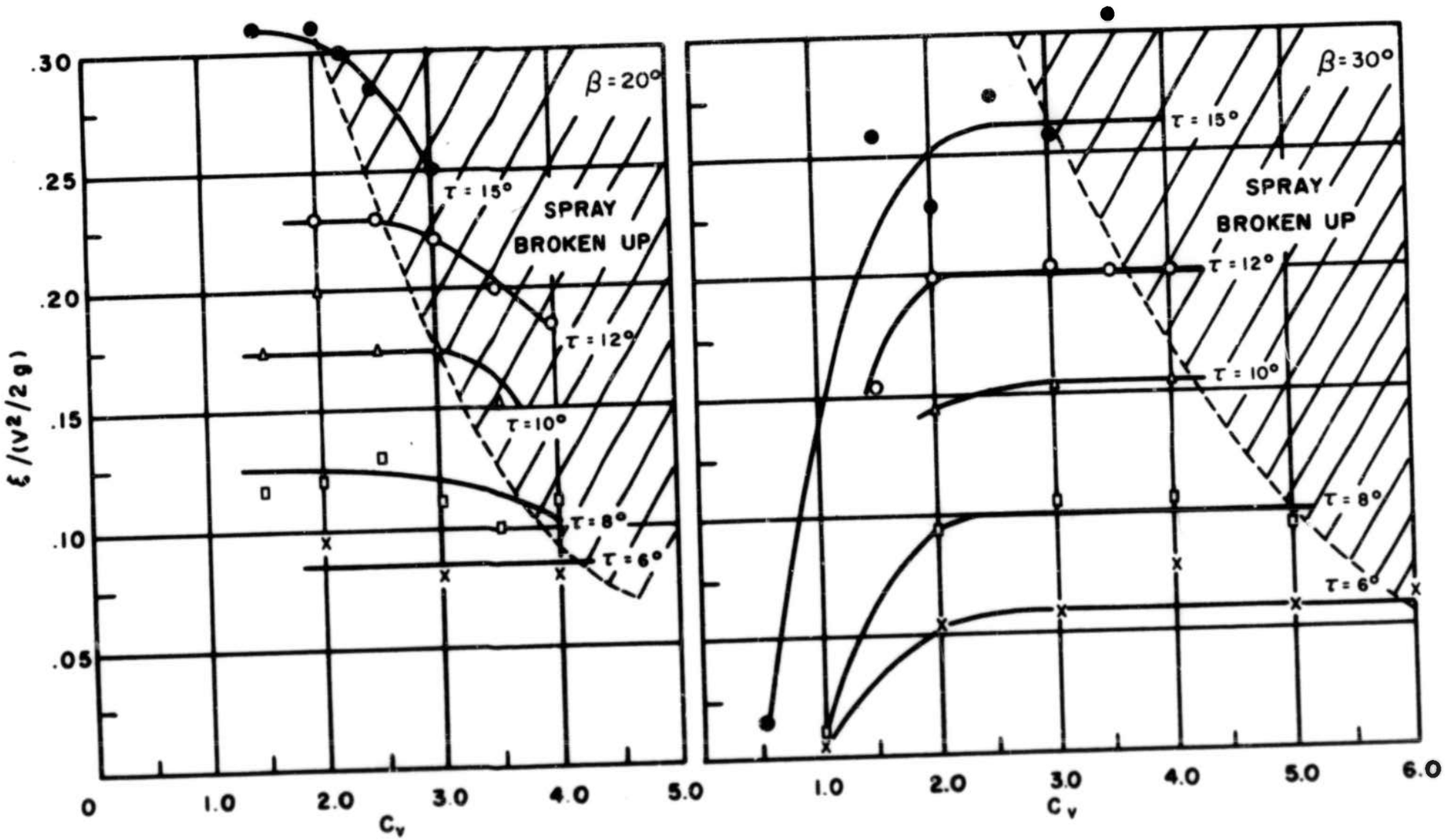

R-678
-39A-

FIGURE 11
VARIATION OF MAXIMUM HEIGHT OF MAIN SPRAY BLISTER
WITH TRIM AND DEADRISE
FOR $C_v > 1.50$

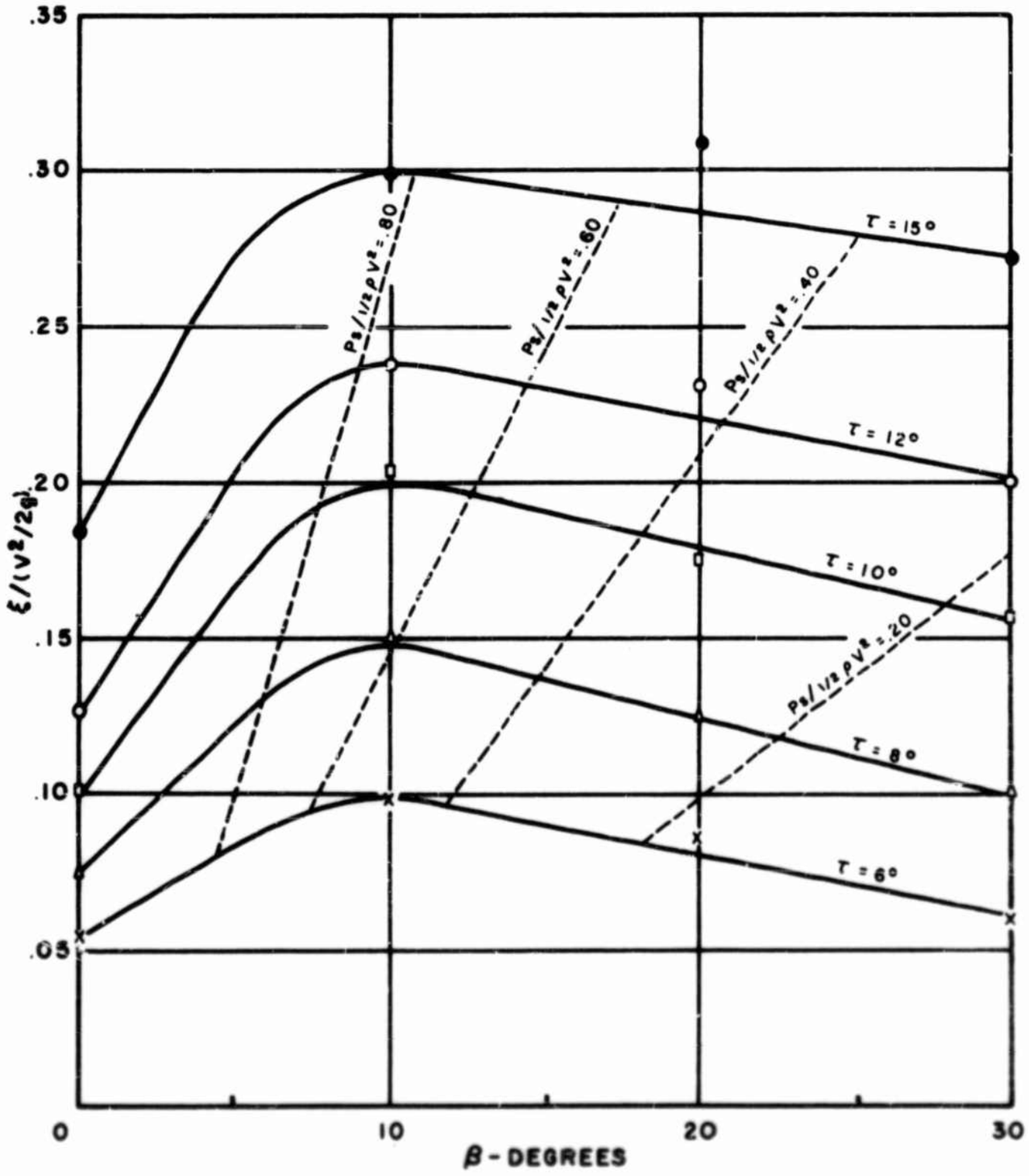

FIGURE 12

VARIATION OF LATERAL POSITION OF MAXIMUM HEIGHT OF MAIN SPRAY BLISTER WITH SPEED COEFFICIENT AND TRIM ANGLE

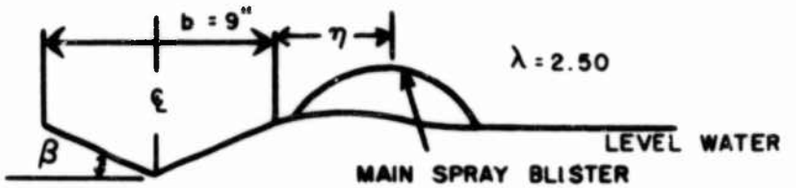

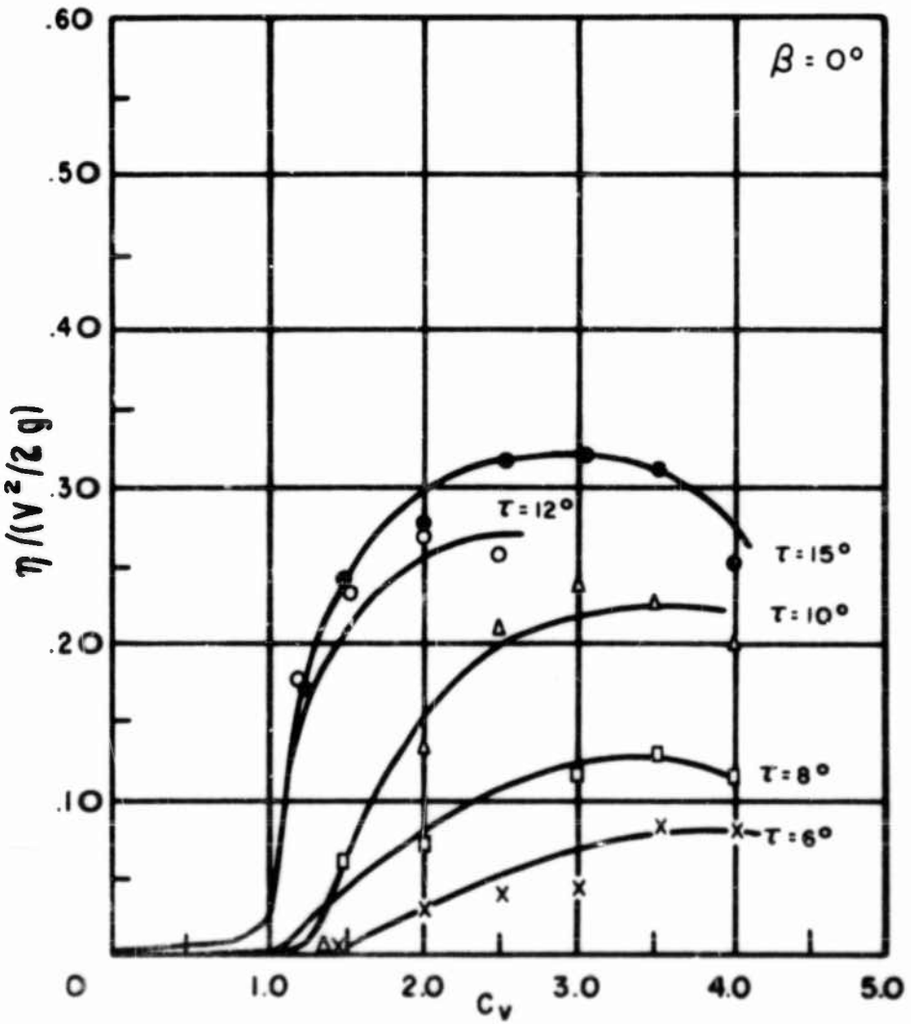

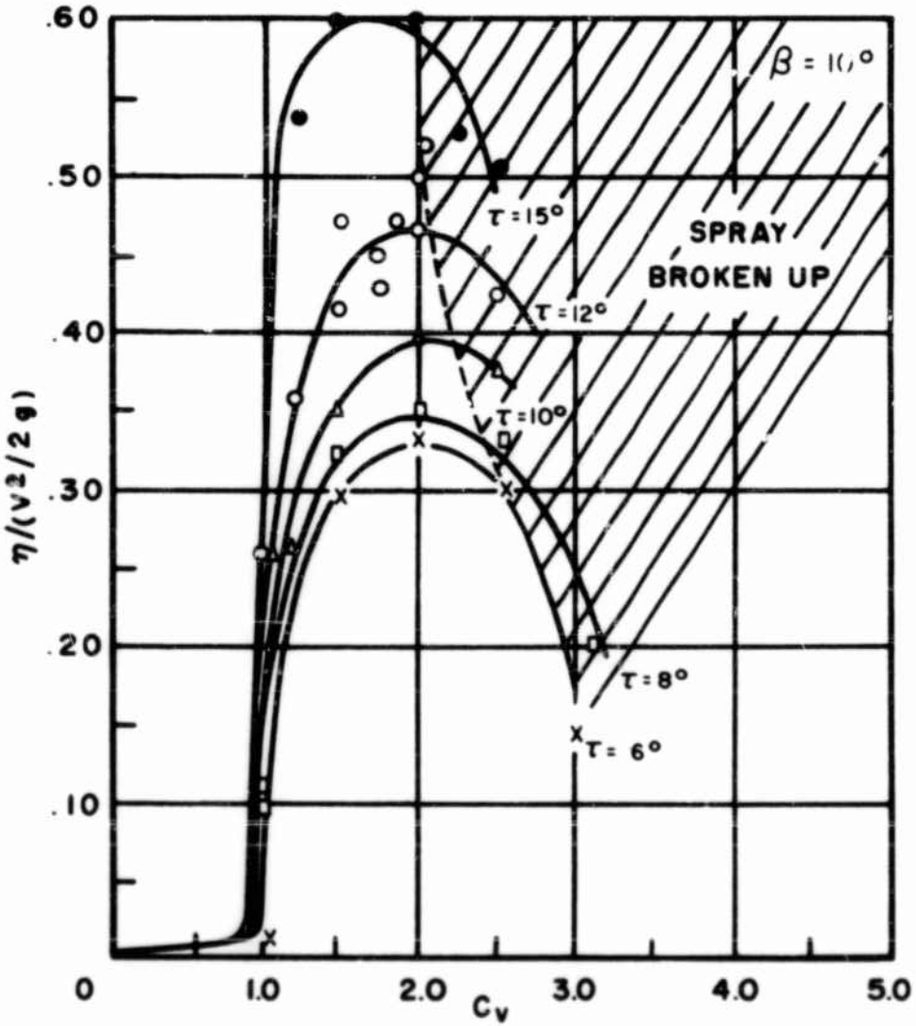

FIGURE 12
(CONTINUED)

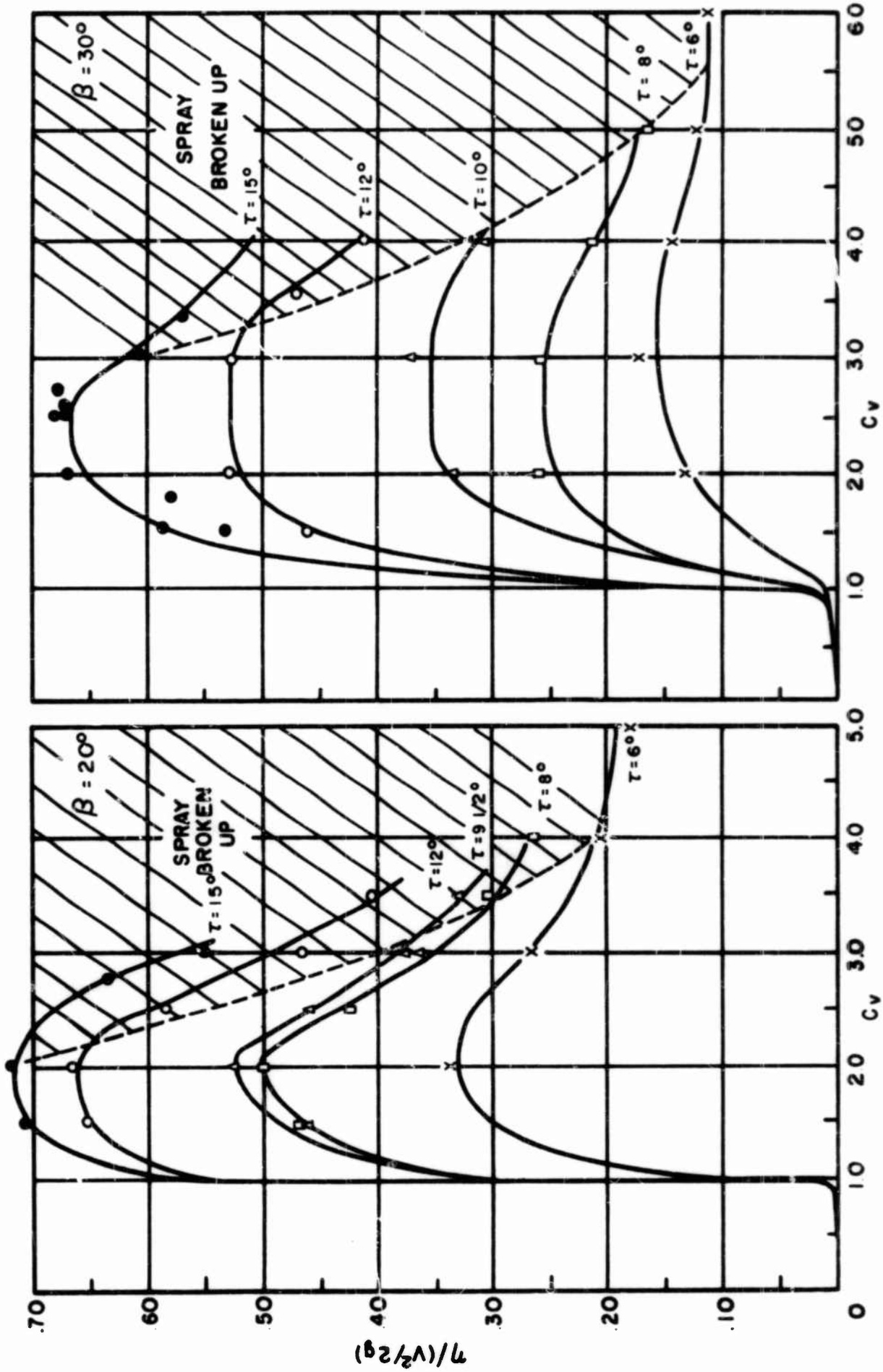

FIGURE 13

VARIATION OF LATERAL POSITION OF MAXIMUM SPRAY HEIGHT WITH TRIM AND DEADRISE

(MAXIMUM LATERAL POSITIONS TAKEN FROM FIGURE 12)

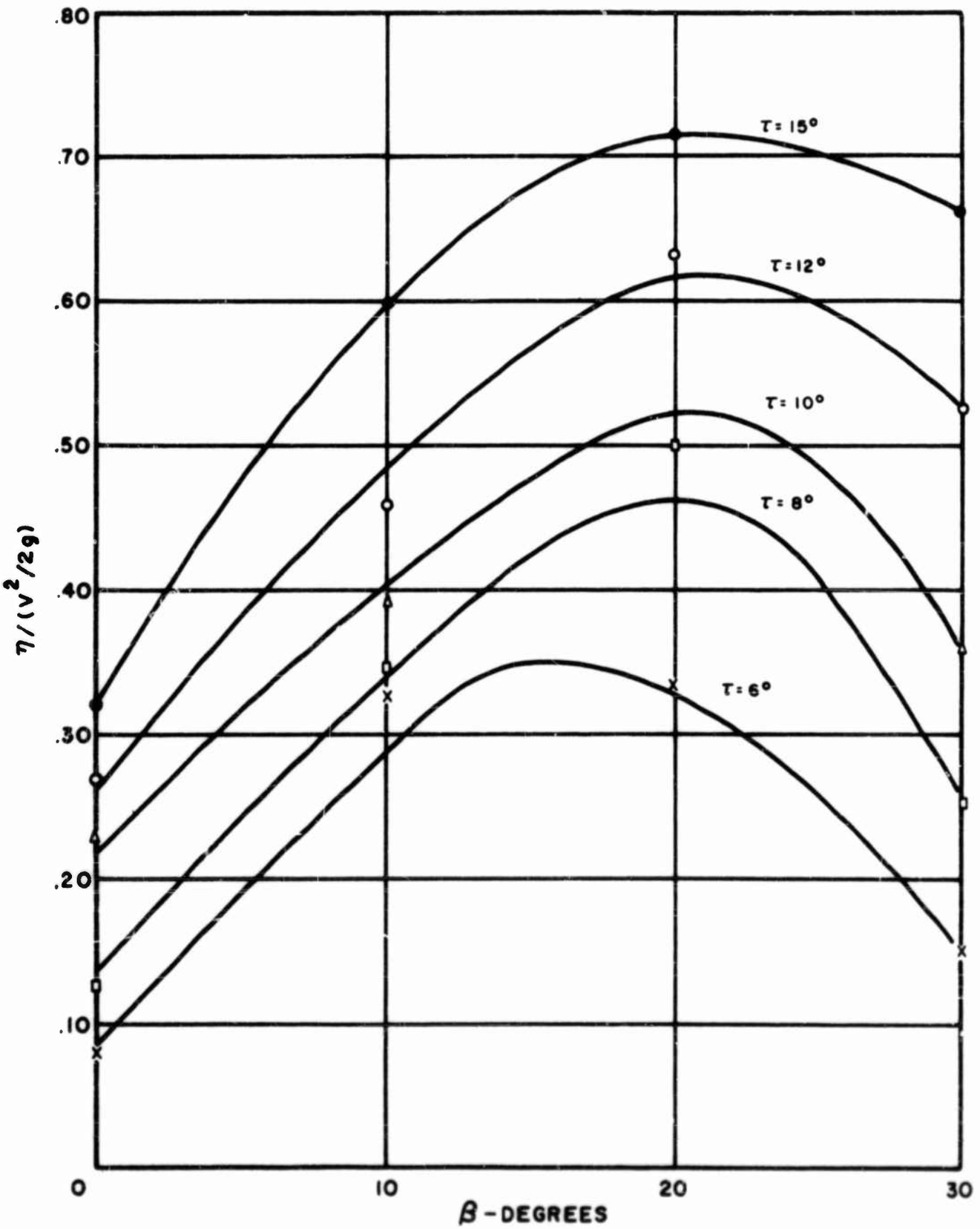

FIGURE 14

EFFECT OF VERTICAL CHINE STRIPS ON HEIGHT OF MAIN SPRAY

($\beta = 20°, b = 9"$)

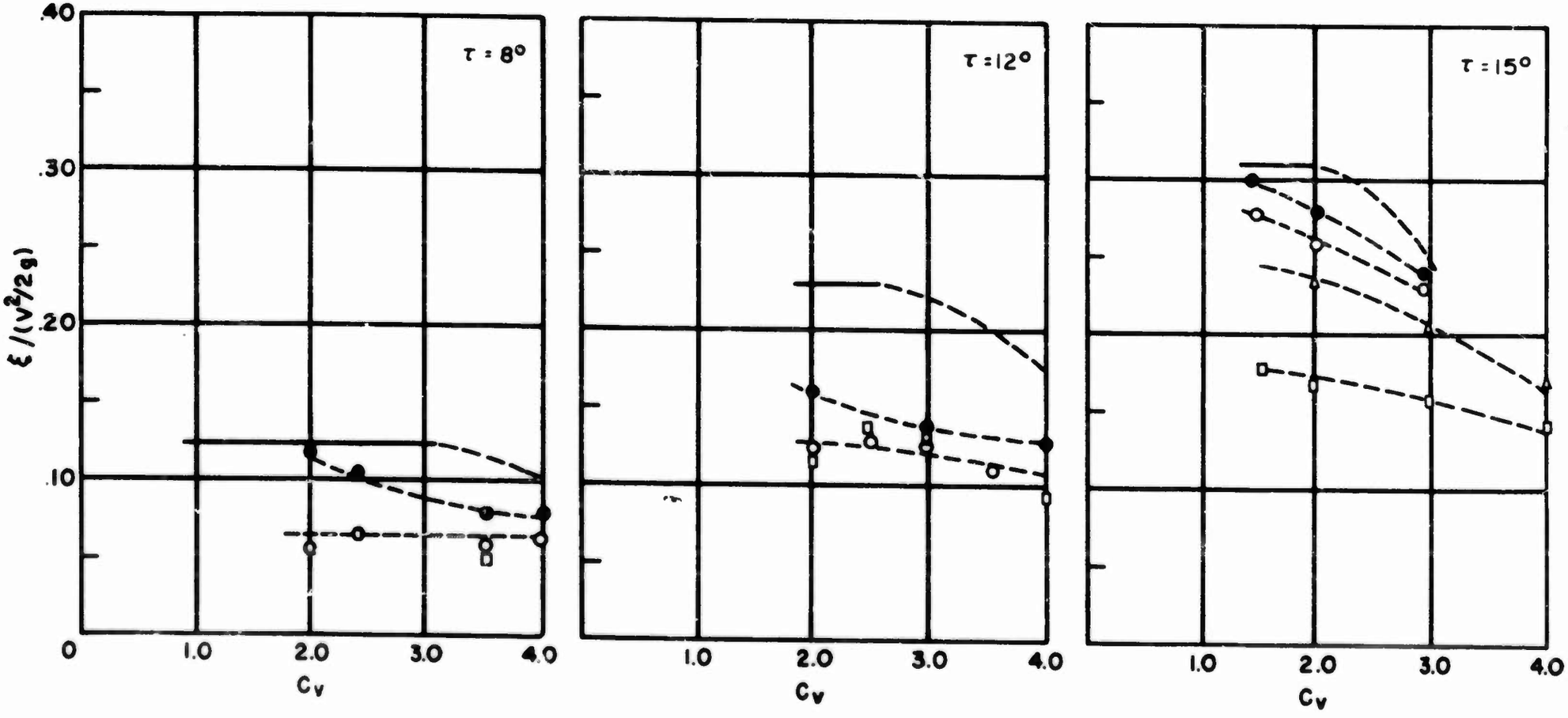

FIGURE 15
EFFECT OF HORIZONTAL CHINE STRIPS ON HEIGHT OF MAIN SPRAY
($\beta = 20^\circ, b=9"$)

d	SYMBOL
O	UNBROKEN BLISTER BLISTER BROKEN-UP
.022b	△
.056b	□